



저작자표시-비영리-변경금지 2.0 대한민국

이용자는 아래의 조건을 따르는 경우에 한하여 자유롭게

- 이 저작물을 복제, 배포, 전송, 전시, 공연 및 방송할 수 있습니다.

다음과 같은 조건을 따라야 합니다:



저작자표시. 귀하는 원저작자를 표시하여야 합니다.



비영리. 귀하는 이 저작물을 영리 목적으로 이용할 수 없습니다.



변경금지. 귀하는 이 저작물을 개작, 변형 또는 가공할 수 없습니다.

- 귀하는, 이 저작물의 재이용이나 배포의 경우, 이 저작물에 적용된 이용허락조건을 명확하게 나타내어야 합니다.
- 저작권자로부터 별도의 허가를 받으면 이러한 조건들은 적용되지 않습니다.

저작권법에 따른 이용자의 권리는 위의 내용에 의하여 영향을 받지 않습니다.

이것은 [이용허락규약\(Legal Code\)](#)을 이해하기 쉽게 요약한 것입니다.

[Disclaimer](#)

Master of Science

**양자 컴퓨팅을 이용한 무선 센서 네트워크에서의
클러스터링 알고리즘 구현**

**Implementation of clustering Algorithms in Wireless
Sensor Network using Quantum Computing**

The Graduate School of the University of Ulsan
Department of Electrical, Electronic and Computer Engineering
Kripanita Roy

Implementation of clustering Algorithms in Wireless Sensor Network using Quantum Computing

Supervisor: Prof. Myung-Kyun Kim

A Master's Thesis

Submitted to
the Graduate School of the University of Ulsan
in partial fulfillment of the requirements
for the degree of

Master of Science

by

Kripanita Roy


Department of Electrical, Electronic and Computer Engineering

University of Ulsan, Republic of Korea

June 2023

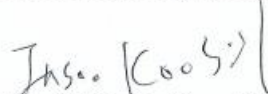
Implementation of clustering Algorithms in Wireless Sensor Network using Quantum Computing

This certifies that the Master's Thesis
of
Kripanita Roy is approved.



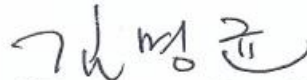
Prof. Dr. Seok-Hoon Yoon

Committee Chair, Dr.



Prof. Dr. In-Soo Koo

Committee Member, Dr.



Prof. Dr. Myung-Kyun Kim

Committee Member, Dr.

Department of Electrical, Electronic and Computer Engineering

University of Ulsan, Republic of Korea

June 2023

ACKNOWLEDGEMENT

I would like to express my sincere gratitude to my thesis advisor, Prof. Dr. Myung-Kyun Kim of the School of Computer Engineering at University of Ulsan for his supervisions, advice, continuous support and constant encouragement throughout my MSc study and related research. I would like to thank my lab mates in the CNLAB laboratory.

I am very much grateful to the University of Ulsan for giving me such a wonderful research environment and financial support. I would like to express my special thanks to Brain Korea 21Plus Program for its contribution and financial support during my study.

Finally, I would like to share a great deal of my achievement with my family and my friends.

Implementation of clustering Algorithms in Wireless Sensor Network using Quantum Computing

by
Kripanita Roy

School of Electrical, Electronic and Computer Engineering
The Graduate School of the University of Ulsan, Ulsan, Korea
(Supervised by Professor Myung-Kyun Kim)

Abstract

Clustering is an effective topology control approach in wireless sensor networks. The majority of the classical clustering algorithm in wireless sensor network requires N steps to select cluster head in an array of N elements. So, CH selection is generally recognized as an NP hard optimization problem which is time consuming and incurs huge computational and data processing times.

In this thesis, we design an optimization strategy that emphasizes adjusting the transmission range according to node density and utilizing a quantum search algorithm to reduce the time complexity associated with selecting the cluster head.

For designing the new clustering topology, we proposed a new classical algorithm that combines necessary parameters such as number of neighbor node, node to node average distance and residual energy with certain weighting factors chosen according to the network system. This thesis considers a fully connected network with a minimum node degree of 1 (i.e., 1-connectivity) to achieve minimum energy consumption and also considered optimum number of clusters by controlling the transmission power. For comparison, we investigated the existing transmission power control topologies such as EECS and HEED. These methods do not address the optimization of transmission power in the whole connected network. Both EECS and HEED use residual energy as a rudimentary factor, as well as intra-cluster communication cost as a secondary factor. However, EECS and HEED show

some drawbacks, increases the network overhead and time complexity. By controlling transmission power, the proposed CH selection mechanism is energy efficient compared to the classical method such as EECS and HEED. Furthermore, the quantum search algorithm used in the method offers a quadratic speedup advantage. It minimizes the time complexity to $O(\sqrt{N})$ compared to classical search algorithm $O(N)$.

In our work, an energy-efficient cluster head selection approach is illustrated through a classical weighted clustering algorithm, and its implementation is also extended through a quantum weighted search algorithm which is demonstrated by the IBM Quantum Qiskit simulation results.

TABLE OF CONTENTS

CHAPTER 01: Introduction	6
1.1 Overview	6
1.2 Thesis Organization	7
CHAPTER 02: Related Work	8
2.1 Clustering Algorithms in Wireless Sensor Network	8
2.2 Quantum Algorithms in Wireless Sensor Network	9
CHAPTER 03: Cluster Head Selection through Classical and Quantum Algorithm	12
3.1 Connectivity of WSN	12
3.2 Energy Model	14
3.3 Expected number of clusters	15
3.4 Classical Weighted Clustering Algorithm	16
3.4.1 Objective of clustering	16
3.4.2 Weighted factors to select cluster head	16
3.4.3 An illustrative Example for Classical Weighted Search Algorithm (CWCA)	19
3.5 3.5.1 Introduction of Quantum Algorithms	22
3.5.1.1 Description of Quantum Search Algorithm	26
3.5.2 Quantum Weighted Search Algorithm	29
3.5.2.1 Basic Complex function for Hamiltonian Construction	29
3.5.2.2 Illustrative example of Quantum Weighted Search Algorithm	31
CHAPTER 4: Performance Evaluation on Classical and Quantum Approach	35
4.1 Classical Approach	36
4.1.1 Transmission Range for fixed network area with different node densities	36
4.1.2 Energy Calculation for intra and cluster head to BS communication	37
4.1.3 Performance evaluation in terms of optimum number of clusters	38
4.2 Quantum Approach	41
4.2.1 IBM Quantum Simulator Results and Discussions	41
CHAPTER 5: Conclusions	45
REFERENCES	47

LIST OF FIGURES

Figure 1	Graphical abstract (3D) of clustering architecture in WSN	6
Figure 2 (a)	Isolated nodes are found	13
Figure 2 (b)	By increasing transmission range r_{tx} , connections are established in the whole network, and no isolated nodes are observed	13
Figure 3	Flowchart of cluster head selection and cluster formation in the CWCA Algorithm	18
Figure 4 (a)	Initial deployment of sensor nodes	19
Figure 4 (b)	Identification of neighbour nodes	19
Figure 4 (c)	An example of the node-to-node distance calculation	20
Figure 4 (d)	Identification of the cluster head using the CWCA	20
Figure 5	Representation of Qubit Bloch Sphere	23
Figure 6	Two qubits in a superposition state	27
Figure 7	Changing the sign of the state to negative	28
Figure 8	Inversion about the mean operation	28
Figure 9 (a)	The relationship between the number of sensor nodes and transmission range.	36
Figure 9 (b)	The number of clusters and transmission range	36
Figure 10 (a)	Optimum number of clusters in Intra-Cluster communication	41
Figure 10 (b)	Optimum number of clusters in CH to BS communication	41
Figure 11 (a)	Initialization of the quantum circuit	42
Figure 11 (b)	Represent Oracle marked states $ 1001\rangle$	42
Figure 11 (c)	Represent Oracle marked states $ 1100\rangle$	42
Figure 11 (d)	The diffusion operator to invert the mean	42
Figure 11 (e)	The complete quantum circuit ready to run on a simulator or quantum system to find the target element with high probability	42
Figure 12 (a)	QasmSimulator results when the number of shots = 1024	43
Figure 12 (b)	QasmSimulator results when the number of shots = 8192	43

LIST OF TABLES

Table 1	The energy model’s parameters and their descriptions	14
Table 2	Calculation of CH selection parameters, and implementation of the CWCA	21
Table 3	Truth table of I-gate	24
Table 4	Truth table of X-gate	24
Table 5	Truth table of Y-gate	24
Table 6	Truth table of Z-gate	25
Table 7	Truth table of Hadamard-gate	25
Table 8	Truth table of CNOT-gate	26
Table 9	Quantum algorithm based on weighted targets parameters and its implementation	32
Table 10	Iterations steps for finding the target nodes	34
Table 11	Transmission range for fixed Network area and different node density. (Probability of connectivity considered 0.99)	36
Table 12	Computation parameters and values	37
Table 13	Energy calculation of Intra cluster communication	38
Table 14	Energy calculation of CH to BS communication	38
Table 15	Computation parameters and values for optimum number of clusters	39
Table 16	Energy calculation of Intra cluster communication in 50 x 50 m ² Area	39
Table 17	Energy calculation of Cluster head to Base Station (CH to BS) communication in 50 x 50 m ² Area.....	40

CHAPTER 1

Introduction

1.1 Overview

For decades, wireless sensor networks (WSNs) have attracted a lot of attention, mostly because of their diverse applications across a wide range of fields. Many military and civilian applications (for example, intelligent transportation systems) integrate tasks such as detection, classification, plus the localization and tracking of events or targets in sensor fields [1–4]. Typically, wireless sensor nodes in networks are organized into several clusters, as shown in Figure 1, and each cluster has a cluster head (CH) that collects information from each member node (sensor) in the cluster and transmits data to the BS as shown in Figure 1.

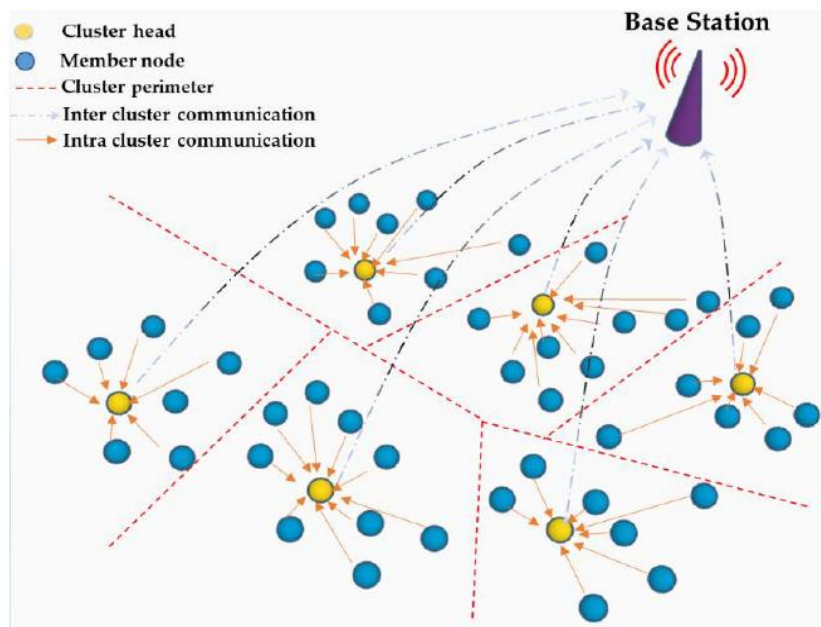


Figure 1. Graphical abstract (3D) of clustering architecture in WSN

In our thesis, we propose a modified CH selection method by assigning an individual weight to each sensor node based on its node degree, the average distance between the CH and its member nodes, as well as this, we assign residual energy as a function of transmission power [5-7]. As mentioned, our work focuses on a homogeneous, randomly connected network, and our goal is energy-efficient CH selection by controlling the transmission power. Two nodes can

communicate directly if their transmission ranges overlap, which signifies the connectivity between them. For multi-hop communications, connectivity is a fundamental property, but because we are concerned with finding the optimum transmission range, we must consider a fully connected network with a minimum node degree (i.e., 1-connectivity)[9-10]. A network with k -connectivity ($k \geq 2$) has much better fault tolerance than a network does with only 1-connectivity, but higher connectivity requires more power consumption [22]. In our thesis, we consider, a fully connected network with a minimum node degree (1-connectivity) to minimize energy consumption. During intra-cluster communications, each node adjusts its transmission power based on the cluster range or radius, instead of transmitting at maximum power. Hierarchical clustering algorithms are based on classical algorithms in which several clusters are formed [24,25]. If the number of clusters and the total number of elements are represented by k and n , respectively, then the time complexity of a hierarchical algorithm is $O(kn^2)$. This time complexity represents time complexity that is similar to NP-hard (non-deterministic polynomial) problems [26]. Hence, CH selection is generally recognized as an NP-hard optimization problem [27,28], and its time complexity is equivalent to $O(kn^2)$ by a classical approach. As a result, the CH selection procedure is also time consuming. Therefore, the main challenge is to overcome time complexity, which incurs huge computational and data processing times. In this thesis, CH selection was proposed via Grover's Quantum Weighted Search Algorithm (QWSA) where the nodes represented as qubit states, allowing it to cover numerous networks with a limited number of qubits.

1.2 Thesis Organization

The rest of the thesis is organized as follows. Chapter 2 describes related works. Chapter 3 describes the methods of clustering algorithms through classical and Quantum approach including the energy models. Then we present the design of the proposed algorithm called CWCA and QWSA algorithm based on target weights to select energy efficient cluster head. Chapter 4 presents a performance evaluation of the proposed classical and quantum algorithms, along with results and a discussion. In Chapter 5, the overall outcomes of this research are summarized in this section. Furthermore, some suggestions for the improvement of this model were also analyzed and discussed for the future work related to this research.

CHAPTER 2

Related Work

2.1 Clustering algorithms in wireless sensor network

Clustering in wireless sensor networks has been an active research area in many years. The goal of clustering is to improve the energy efficiency and performance of the network by reducing the amount of communication overhead required for nodes to communicate with each other and with the base station. Cluster heads play a critical role in clustering algorithms as they perform crucial tasks such as data aggregation, resource allocation, network management, routing, and security [10-12]. So, cluster head selection is important to handle the limited energy in the best possible way to uplift the network lifetime.

The most commonly used clustering protocol is Low Energy Adaptive Clustering Hierarchy (LEACH) [19]. The probability of selecting the CH in LEACH is a totally random process with no guarantee of the number of CHs, which adversely affects the overall performance of the network. Power-Efficient Gathering in Sensor Information Systems (PEGASIS) [36] is an improvement over the LEACH protocol. The fundamental idea behind PEGASIS is for each node to communicate with and send data to its immediate neighbors, while they take turns acting as the leader, transmitting to the BS. The nodes arrange themselves into a chain by using a greedy algorithm. The data transmission is direct between the leader and the BS within a fixed transmission range. However, an adjustment of the transmission power level in the whole network is not discussed. On the other hand, transmission-power-based protocols such as EECS [20] and HEEDS [21] use residual energy as a rudimentary factor, as well as intra-cluster communication cost as a secondary factor. Under EECS, a candidate node that is going to become a CH needs to ensure that its residual energy is within radio range R_{compete} . But this radio range is inversely proportional to the square root of k_{opt} , which is the optimal range of the CH. The optimal range selection equation is taken from the LEACH protocol, but there is no control of optimum transmission power. To resolve this problem, the selection of an optimal number of clusterheads is proposed in this thesis work, while managing optimum transmission power. On the otherhand, in the EECS cluster formation phase, a complex cost function for distance prioritizes only the cluster-head-to-BS distance, which eventually increases the

overhead and time complexity in the whole network. The total control of the given overhead complexity is $O(N)$, and to overcome this, we propose a quantum algorithm for CH selection where the overhead complexity is reduced to $O(\sqrt{N})$. Author of [8] Hybrid Energy-Efficient Distributed (HEED) protocol considers CH selection based on the ratio of the estimated current residual energy in a sensor node and its maximum energy. Transmission power level control can be optimized by setting one specific cluster power level for intra- and inter-cluster communications. The connectivity requirement setting cluster range $R_t \sim \sqrt{\frac{\log n}{n}}$ (where n is the total number of nodes) is for a unit square region in intra-cluster communications. However, the probability of connectivity in the whole network does not consider any specific limit on the transmission range. To resolve this issue, we studied minimum network connectivity where at least one node in the network can connect to achieve the optimum transmission power level depending upon node density. Another important point is to consider the time complexity, which is $O(N)$ per node under this protocol. The author in [38] proposed, Energy-Efficient Cluster Formation (EECF) a distributed clustering protocol that considers the node degree and residual energy for cluster head election. There is no mention of re-adjusting the transmission power level during each round, but a fixed transmission range for at least one cluster head cannot guarantee efficient communications. Like EECS, EECF has a worst-case algorithmic complexity of $O(N)$ at each node.

2.2 Quantum Algorithm in wireless sensor network

Quantum computing becomes a commercial reality, it may be used in wireless communications systems in order to speed up specific processes due to its inherent parallelization capabilities. While a classical bit may adopt either the values 0 or 1, a quantum bit, or *qubit*, may have the values $|0\rangle, |1\rangle$ or any superposition of the two [9], where the notation $|\cdot\rangle$ is the ket representation [23] and it is the column vector of a quantum state. If two qubits are used, then the composite quantum state may have the values $|00\rangle, |01\rangle, |10\rangle$ and $|11\rangle$ simultaneously. In general, by employing b bits in a classical register, one out of 2^b combinations is represented at any time. By contrast, in a quantum register associated with b qubits, the composite quantum state may be found in a superposition of all 2^b values simultaneously. In this thesis, we will focus our attention on the employment of quantum

algorithms in classical communication systems.

The problem of Cluster head selection in classical clustering algorithm is one of the interesting topics studied recently. In classical clustering algorithm, CH selection is generally recognized as an NP-hard optimization problem. The number of clusters and the total number of elements are represented by k and n , respectively, then the time complexity of a clustering algorithm is $O(kn^2)$. This time complexity represents time complexity that is similar to that of NP-hard (non-deterministic polynomial) problems [26]. As a result, the CH election procedure is also time consuming.

In order to improve on the time complexity problem, quantum algorithms can play significant roles. Recently, CH selection was proposed via the Quantum Approximate Optimization Algorithm (QAOA) [29]. The QAOA structure is classified into two parts: parameterization and classical optimization. A parameterized quantum circuit consists of building a Hamiltonian problem where the proper optimization of the parameters is essential [30]. In a parameterized quantum circuit, the components of the circuit are demonstrated by δ and the output state $|\phi(\delta)\rangle$. The Quantum Max Cut problem solved by the QAOA needs to optimize the circuit parameters efficiently [31]. The main problem of the QAOA algorithm is that it considers each qubit (q_i) as an individual node, which unintentionally limits it from forming clusters in the whole network. For instance, IBM's 127-qubit Eagle is the biggest quantum computer, yet it has only 127 qubits. Consequently, the highest number of network nodes that can be used is only 127. For a larger network (>127), the above-mentioned QAOA algorithm is impractical.

To overcome this issue, in this thesis, we conduct the CH selection technique based on the Quantum Search Algorithm (QSA) using weighted targets [32,33]. The platform of the QSA is related to Grover's search algorithm. According to Panchi et al. [34], the probability of obtaining each search target is equal in the traditional quantum search algorithm. In order to resolve this problem, they proposed a weighted target-based quantum search algorithm where the probability of finding each target resembles the corresponding weight coefficient, and it is constituted as a quantum superposition state. If all the sensor nodes are assigned by an individual weight, then it is possible to apply the weighted-based QSA algorithm to select the appropriate cluster head. In addition, we apply this algorithm to select a CH, which efficiently

improves the time complexity compared to that of the classical approach. This weighted approach to Grover's search algorithm has time complexity $O(\sqrt{n})$, where n is the number of search items or, in our case, the total number of sensor nodes in the whole network and it is quadratically outperforms the classical counterparts in terms of time.

CHAPTER 3

Cluster head selection through Classical and Quantum Algorithm

3.1 Connectivity of WSN

In wireless sensor network, each node is independently and randomly placed in a two-dimensional simulation area (A). uniform random distribution is used such that for a large network (n) and a large area (A), we can define a constant node density, $\rho = \frac{n}{A}$ which denotes the expected number of nodes per unit area. A radio link model is assumed in which each node has a specific transmission range to represent wireless communications between the nodes. If two nodes are within range of one another, they can directly communicate through a wireless link. To establish connectivity in the whole network, a necessary condition is that each node has at least one neighbor node ($d_{min} > 0$) [9]. If the node degree is defined by $d(n)$, then the minimum node degree of a network is denoted as:

$$d_{min}(N) = \min \{d(n)\} \quad (1)$$

Therefore, a node is considered to be isolated if $d = 0$. From the definition of a k connected network, each node pair has at least k mutually independent path(s) ($k = 1, 2, 3 \dots$) and the probability of that network is indicated with $P(k\text{-con})$. In our analysis, we consider $k = 1$ to represent the probability of a 1-connected network, $P(1\text{-con})$, so a network is steadily connected if $P(1\text{-con}) \geq 0.95$ [43]. Because we are interested in finding the optimum transmission power for the whole network, it is dependent on the distributed node density (ρ) and the node degree ($d_{min} > 0$). If no node is isolated, then the transmission range (r_0) can be represented as a function of node density and probable node degree, as proposed by Bettstetter [22].

$$P(d_{min} > 0) = P_{non-iso} = \prod_{u=1}^N P_{non-iso} = (1 - e^{-\rho\pi r^2})^N \quad (2)$$

The transmission range of each node is denoted with r_{tx} . By adding \ln to both sides of Equation (2), we can determine the transmission range as follows [22]:

$$r_{tx} = \sqrt{\frac{-\ln(1 - P_{non-iso}^{\frac{1}{n}})}{\rho\pi}} \quad (3)$$

The significance of this equation is demonstrated by the following example.

Example 1: Consider a network of totally deployed sensor nodes, $n = 100$, in a square area, $A = 100 \text{ m} \times 100 \text{ m}$, which yields a node density of $\rho = \frac{N}{A} = \frac{100}{100 \times 100} = 0.01 \text{ m}^{-2}$.

If the probability of connectivity is $P = 0.94$, then the transmission range r_{tx} can be calculated with Equation (3):

$$r_{tx} = \sqrt{\frac{-\ln(1 - 0.94^{\frac{1}{100}})}{0.01 * \pi}} = 15.0 \text{ m}$$

If the transmission range $r_{tx} = 15 \text{ m}$, then Figure 2a depicts two nodes that are isolated. In order to connect at least one of those nodes, the transmission range needs to be modified. For this reason, the probability of connectivity needs to be $p \geq 0.95$ to reconnect the nodes. Here, we consider $p = 0.99$. Therefore, the modified transmission range will be:

$$r_{tx} = \sqrt{\frac{-\ln(1 - 0.99^{\frac{1}{100}})}{0.01 * \pi}} = 17.0 \text{ m}$$

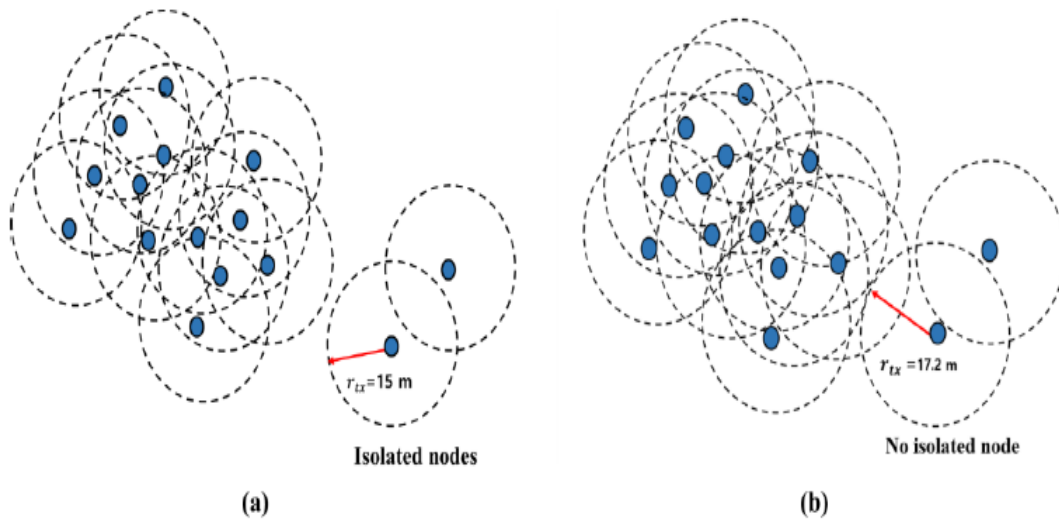


Figure 2. (a) Isolated nodes are found. (b) By increasing transmission range r_{tx} , connections are established in the whole network, and no isolated nodes are observed.

After increasing the transmission range to 17.12 m, as shown in Figure 2b, the whole network is connected. Therefore, the node degree and the node density are considered in designing an adjustment model of the transmission range to establish an energy efficient network with full reachability.

3.2 Energy Model

We used a simplified energy model shown in [15] for radio hardware energy dissipation transmitting an l-bit message (E_{TX}) with distance d as follows:

$$E_{TX}(l, d) = \begin{cases} l * E_{elec} + l * \epsilon_{fs} * d^2; & d \leq d_0 \\ l * E_{elec} + l * \epsilon_{mp} * d^4; & d \geq d_0 \end{cases} \quad (4)$$

All parameter descriptions are in Table 1.

Table 1. The energy model's parameters and their descriptions.

Parameters	Description
E_{elec}	Energy required to run the transmitter or receiver
ϵ_{fs}	Amplifier's power loss for a short distance called free space
ϵ_{mp}	Amplifier's power loss for a long distance called multipath fading
$d_{non-CH \text{ to } CH}(d^2)$	Distance from non-CH to CH
$d_{CH \text{ to } BS}(d^4)$	Distance from CH to BS
$d_0 = \sqrt{\frac{\epsilon_{fs}}{\epsilon_{mp}}}$	Threshold Transmission Distance
E_{DA}	Data Aggregation

When receiving data, the radio expends the following [35]:

$$E_{RX}(l) = l * E_{elec} \quad (6)$$

Additionally, the energy dissipated by the cluster head during a single frame is:

$$E_{CH} = l * E_{elec}(m-1) + lE_{DA} m + l * E_{elec} + l * \epsilon_{mp} d^4 \quad (7)$$

Assuming that there are N nodes which are distributed uniformly, if there are k clusters, then on the average number of nodes per cluster, $m = \frac{N}{k}$. Each CH dissipates. energy by receiving signals from the nodes, collecting the signals, and transmitting the gathered signals to the BS. The energy required in each non-cluster-head node can be expressed by [35]:

$$E_{non-CH} = l * E_{elec} + l * \epsilon_{mp} d^2 \text{ to } CH \quad (8)$$

3.3 Expected number of clusters

Before the selection of the CH, it is necessary to define the expected number of clusters in the network. Using the following computation and connectivity model, we analytically estimate the expected number of clusters (k_{opt}). Let us assume there are N nodes which are distributed uniformly in area A. The nodes are stationary, and therefore, the density is constant. The transmission area of a sensor node can be assumed to be $A_s = \pi r_{tx}^2$, where r_{tx} is the transmission range of the sensor node (from Equation (3)). As mentioned, before, transmission range depends on node connectivity and density, and using these two assumptions, the expected number of clusters, $E_n = \frac{A}{A_s}$.

An illustrative example is given to clarify the above assumptions: nodes n = 100, and area, A = 100 m x100m. Because the nodes are stationary, the node density $\rho = \frac{n}{A} = 0.01 m^{-2}$. From Example 1, we already found that our expected transmission range is 17.12 m. The transmission area of one sensor node will be $A_s = \pi r_{tx}^2 = [3.1416 \times (17.12)^2] = 921 m^2$. Now, we must calculate the expected number of clusters by dividing the entire sensing. area through the obtained transmission area:

$$\text{Expected number of clusters, } E_n = \frac{100 \times 100}{921} \approx 10$$

3.4 Classical Weighted Clustering Algorithm

3.4.1 Objective of clustering

Based on the preceding assumptions, in this work, an algorithm called the classical weighted clustering algorithm (CWCA) is proposed to efficiently combine the necessary parameters, such as the node degree, node-to-node average distance, and current residual energy, with certain weighting factors being chosen according to the network system. In wireless networks, for instance, power regulation is crucial, and hence, the weight of the corresponding parameter might be larger. The adaptability from altering the weighted variables enables us to apply this proposed method across different networks. A predefined value threshold for node degree needs to be set in the clusters to ensure that the cluster heads are not encumbered, and that throughput is achieved by optimizing the number of member nodes of each cluster head (the node degree). In addition, the battery power of a sensor node needs to be effectively utilized within a particular transmission range; for instance, communication between the nodes will use less power if they are close to one another. Since a CH is responsible for additional tasks, it uses more battery power than an ordinary node does. It can interact more smoothly with the neighbors within the transmission range and those located closer to it. Due to signal attenuation, communication between the nodes and the CH becomes challenging as the distance increases.

3.4.2 Weighted factors to select cluster head

Considering weighted factors such as node degree, node average distance and energy consumption, the CH selection procedure consists of the following steps.

Step 1: Within transmission range, find the neighbors of each node, s , which define their node degree, d_s , as follows:

$$d_s = |N(s)| = \sum_{n \in S} \{dist(s, n) < r_{tx}\} \quad (9)$$

where d_s , represent the degree of each sensor node s ; S = the set of sensor nodes; n = the neighbors of sensor node s ; r_{tx} = the transmission range of sensor node s .

Step 2: Evaluate the degree difference, d_f for every node :

$$d_f = |d_s - \gamma| \quad (10)$$

where d_f =the current node degree of the sensor node, and γ = the expected or predefined node degree.

Step 3: Compute the sum of the distances of the member nodes within the transmission range, and find the average distance, D_{avg}

$$D_s = \sum_{n \in S(s)} \{dist(s, n)\} \quad (11)$$

$$\text{Average distance, } D_{avg} = \frac{\sum D_s}{d_s}$$

Step 4: Compute the residual energy to find the node with the highest energy level:

$$E_s = 1 - \frac{E_{re}(s)}{E_i(s)} \quad (12)$$

Where $E_{re}(s)$ = the residual energy of node s, and $E_i(s)$ = the initial energy of node s.

Step 5: Calculate combined weight, W_s for each node s which might become a CH. The lowest weighted node will be chosen as CH:

$$W_s = w_1 \Delta s + w_2 D_{avg} + w_3 E_s \quad (13)$$

where w_1 , w_2 , and w_3 are the weight factors for the corresponding system parameters. The node with the minimum weight will be selected as the cluster head, so:

$$w_1 + w_2 + w_3 = 1 \quad (14)$$

The first component, Δs , or the node degree difference, is the important factor for a CH in order to control several nodes in its cluster. This also ensures that the CH is not overloaded, and the efficiency of the system is retained at the intended level. The second component D_{avg} is mainly related to energy consumption because more power is required to communicate over a larger distance. It is important to find the node which is located at the center of a cluster. The last component, E_s , contemplates a sensor node's available battery power. The CH battery

drainage will occur quickly compared to that which occurs in other nodes. Within the transmission range, each node compares its energy level with the other nodes. The node with the highest energy level has an increased probability of becoming the CH. Overall, this term is dependent on the node's starting power along with the power needed over time based on the network traffic.

The flowchart for the proposed cluster head selection is presented in Figure 3.

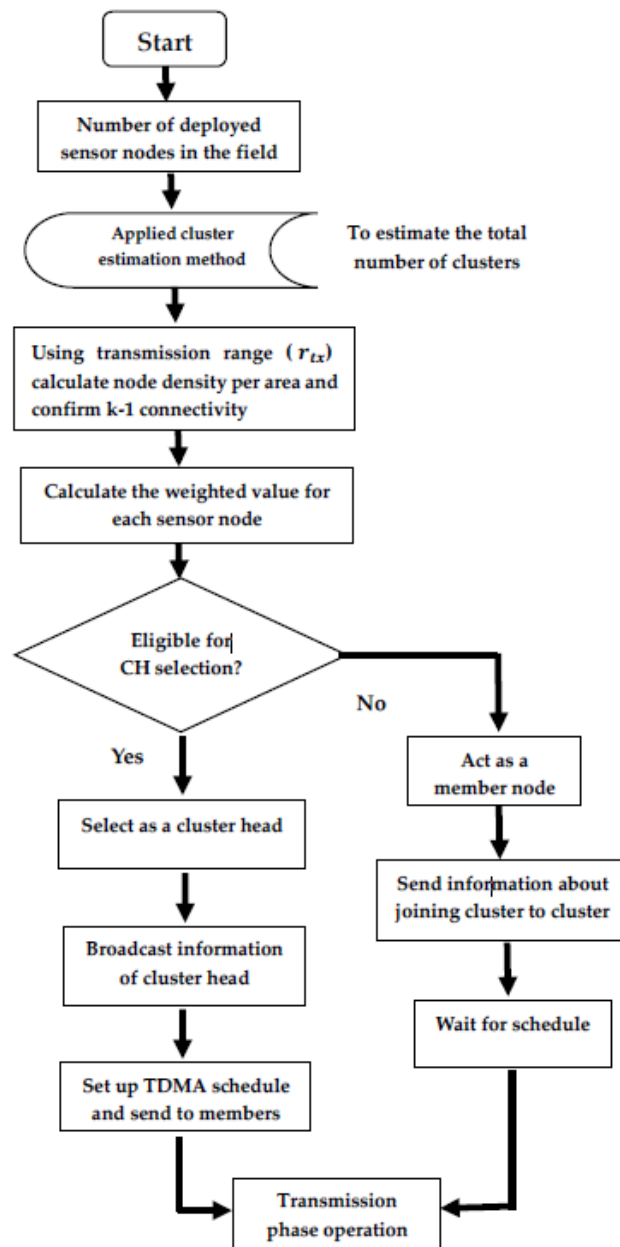
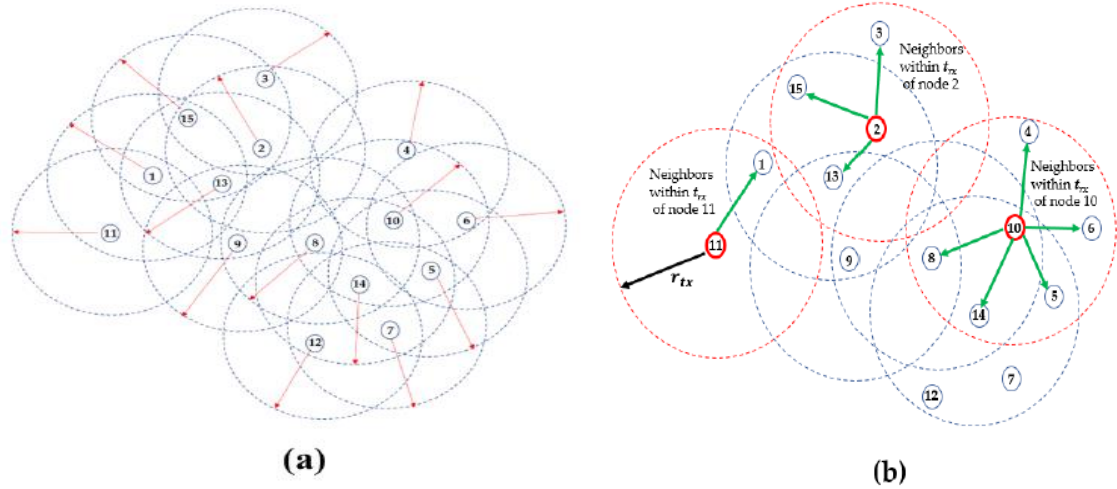


Figure 3. Flowchart of cluster head selection and cluster formation in the CWCA algorithm.

3.4.3 An illustrative example for CWCA Algorithm

In our proposed classical weighted algorithm, we assume that 15 nodes are initially deployed in an area 50 m x 50m, as shown in Figure 4a. The red arrow shows each node's transmission range (r_{tx}), which is equal for all of the nodes, and the dotted circles represent the transmission area (A_s). Figure 4b identifies the neighbor(s) of sensor nodes within the transmission range r_{tx} . For instance, node 11 has only one neighbor within the transmission range r_{tx} , whereas node 10 and node 2 have five and three neighbor nodes, respectively. Therefore, in Table 2, the current node degree d_s , is calculated according to Figure 4b. The degree difference is important and needs to be set, otherwise, some clusters will be heavily loaded, and others will be lightly loaded. To quantitatively determine the well-balanced clusters in our algorithm, we use the following expression for degree difference: γ = the expected node degree.

$$\gamma = \frac{N - k_{opt}}{k_{opt}} \quad (15)$$



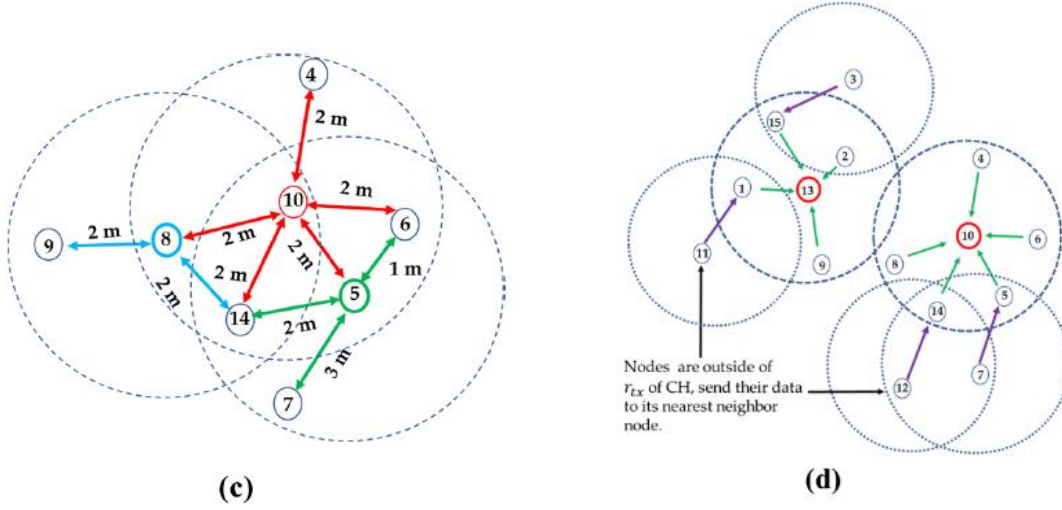


Figure 4. (a) Initial deployment of sensor nodes; (b) identification of neighbor nodes, (c) an example of the node-to-node distance calculation; (d) identification of the cluster head using the CWCA.

In this example, the total number of nodes $n = 15$, the area $A = 50 \text{ m} \times 50 \text{ m}$, and the node density $\rho = \frac{n}{A} = \frac{15}{2500} = 0.006 \text{ m}^{-2}$. Hence, no node is isolated, based on Figure 4a, and the probability of connectivity will be 99%. Now, we can determine that our expected transmission range from Equation (3) is 20 m. Therefore, the transmission area of each sensor node ($A_s = \pi r_{tx}^2$) will be 1256 m^2 . The expected number of clusters (k_{opt}) for area A can be computed as $E_n = \frac{50 \times 50}{1256} \approx 2$. From Equation (15), we calculate the expected node degree difference (γ) as 6.5~7. The sum of the distances, D_s , for each sensor node is shown in Figure 4c, where the unit distance was chosen randomly. To ensure that the probable location of the CH is in the center, we consider the average distance, D_{avg} , instead of taking the sum of D_s . Because long-distance communication consumes more energy, D_{avg} minimizes the intra-cluster communication energy consumption. In the next step, we calculate residual energy $E_{re}(s)$ for the candidate cluster heads. Now, in the final step, the minimum weighted node will be selected as the CH.

The weighting factors which are assumed in order to calculate total weights in Table 2 are $w_1 = 0.7$, $w_2 = 0.2$, and $w_3 = 0.1$ [44]. We note that weighting factors are chosen randomly, such

that $w_1 + w_2 + w_3 = 1$. This is basically used to normalize the appropriate combination of weighting factors, such as the degree difference, the distance from neighboring nodes, and the energy usage. By adjusting the weighting factors, the combination of various eligibility requirements can be set in a suitable way. In our example, node degree has the highest priority as a result, so the weight $w_1 = 0.7$ is chosen to represent the node degree. In this experiment, each node begins with only 1 J of energy. Therefore, the energy ratio is one, as depicted in Table 2 for all of the nodes. From Table 2, the lowest weighted nodes, which are node no. 10 and node no. 13, will be selected as the cluster heads. It is worth mentioning that no two cluster heads are adjacent neighbors. We found that all member nodes of each cluster are quite close to the desired node degree set earlier: $\gamma = 7$. Figure 4 (d) clearly identifies the CHs and the member nodes. The member nodes that are outside of the selected cluster head's transmission range (nodes 11, 3, 12, and 7) will send their data to the nearest neighbor node within the transmission range.

Table 2. Calculation of CH selection parameters, and implementation of the CWCA.

Node ID	Current node degree; d_s	Current & expected node degree difference. $d_f = d_s - \gamma $ ($\gamma = 7$)	Normalized value of node degree difference $\Delta s = \frac{ d_s - \gamma }{\gamma}$	(Sum of all member node distance) $\sum D_s$	Average distance $D_{avg} = \frac{\sum D_s}{d_s}$	Energy ratio $E_s = \frac{E_{re}(s)}{E_i(s)}$	Total Weight W_s
1	3	4	0.57	11	3.67	1	1.23
2	3	3	0.43	12	4	1	1.20
3	2	5	0.71	10	5	1	1.60
4	2	5	0.71	15	7.5	1	2.10
5	4	3	0.43	9	2.25	1	0.85
6	2	5	0.71	3	1.5	1	0.90
7	4	3	0.43	16	4	1	1.20
8	3	4	0.57	6	2	1	0.90
9	2	5	0.71	12	5	1	1.60
10	5	2	0.29	10	2	1	0.70
11	1	6	0.86	6	6	1	1.90
12	2	5	0.71	11	5.5	1	1.70
13	4	3	0.43	7	1.75	1	0.75
14	5	2	0.29	12	2.4	1	0.78
15	3	4	0.57	13	4.33	1	1.37

3.5.1 Introduction of Quantum Algorithms

Qubit: Before discussing the concept of quantum algorithm, we need to discuss about quantum computing and its fundamental element defined as “qubit”. A classical computer takes a single unit of information which has a value of either 0 or 1 (off or on, false or true, low or high). The device operates by using logical gates (AND, OR, NOT) to manipulate binary digits (bits) and perform computations. In quantum computers, data is stored in quantum bits, or qubits. Qubits is the fundamental unit in quantum information science. To distinguish between a bit and a qubit, Dirac notation is used to represent the states of the qubit that is $|0\rangle$ and $|1\rangle$.

To get a clear indication of qubit, the state of a qubit is generally represented as an array or a vector as follows:

$$|0\rangle = \begin{bmatrix} 1 \\ 0 \end{bmatrix}$$

And the second vector is given as follows:

$$|1\rangle = \begin{bmatrix} 0 \\ 1 \end{bmatrix}$$

The main difference between qubit and classical bit is that a qubit is always a linear combination of basis states. Qubits are always in a superposition of $|0\rangle$ and $|1\rangle$ that can be represents by the following equation:

$$|\psi\rangle = \alpha|0\rangle + \beta|1\rangle$$

Where α and β are complex number and their sum of the magnitude is equal to 1.

$$|\alpha|^2 + |\beta|^2 = 1$$

The visualization of a qubit and its states can be done by Bloch sphere. The Bloch sphere is generally used as a geometrical representation of the qubit, which is a three-dimensional ordinary space. For details analysis, we can consider Figure 5.,

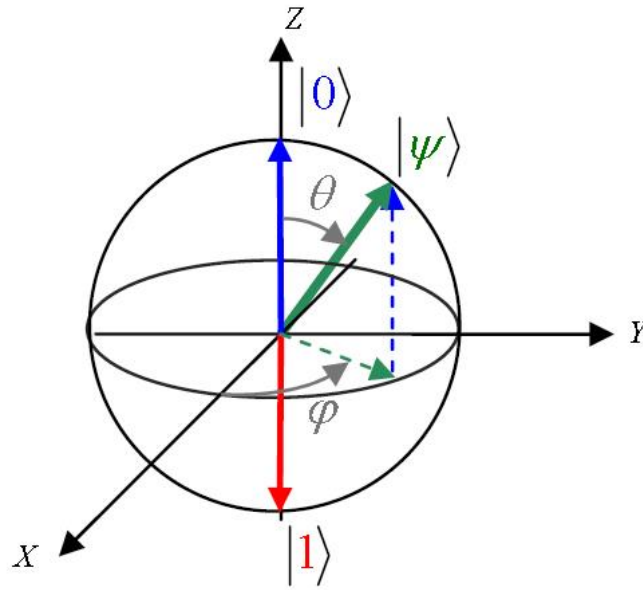


Figure 5 : Representation of Qubit Bloch Sphere [Ref .52]

The north pole and the south pole of the Bloch Sphere represents the $|0\rangle$ state $|1\rangle$ state respectively. The vector rotation along the Bloch sphere can be represented by below:

$$|\psi\rangle = \cos\left(\frac{\theta}{2}\right)|0\rangle + (\cos(\varphi) + i\sin(\varphi))\sin\left(\frac{\theta}{2}\right)|1\rangle$$

Where, θ and φ have the limits $0 \leq \theta \leq \pi$ and $0 \leq \varphi < 2\pi$; θ represents the colatitude to the z axis and φ represents the longitude from the x-axis.

Quantum Logic gates: The basis states of a qubit can be demonstrated as column vector. The basis vector $|0\rangle$ and $|1\rangle$ can be represented as follows:

$$|0\rangle = \begin{bmatrix} 1 \\ 0 \end{bmatrix} ; |1\rangle = \begin{bmatrix} 0 \\ 1 \end{bmatrix}$$

By applying the concept of the basis vector, other necessary logic gates can be constructed. The four basic logic gates for representation of a single qubit are commonly referred to Pauli matrix gates. They are defined as 2×2 complex matrix and represented by the Greek letter sigma ($\sigma_0, \sigma_x, \sigma_y, \sigma_z$). Here we briefly discuss those gates and their truth tables.

The I gate or identity gate action on qubit does not change states which is similar with identity matrix. The equation can be given as follows:

$$I = \sigma_0 = \begin{pmatrix} 1 & 0 \\ 0 & 1 \end{pmatrix}$$

The truth table of the identity gate is given as below:

Table 3– Truth table represent I-gate:

Input	Output
$ 0\rangle$	$ 0\rangle$
$ 1\rangle$	$ 1\rangle$

The X gate or NOT gate moves the state vector from one basis state to the other that is represented by the Pauli X-gate operator as follows:

$$X = \sigma_x = \begin{pmatrix} 0 & 1 \\ 1 & 0 \end{pmatrix}$$

The following truth table describes the operation rotation around the x axis:

Table 4– Truth table represent X-gate:

Input	Output
$ 0\rangle$	$ 1\rangle$
$ 1\rangle$	$ 0\rangle$

The Y gate is a rotation around the y axis by 180 degree which is shown as below:

$$Y = \sigma_y = \begin{pmatrix} 0 & i \\ i & 0 \end{pmatrix}$$

The following truth table describes the operation rotation around the y axis:

Table 5– Truth table represent Y-gate

Input	Output
$ 0\rangle$	$i 1\rangle$
$ 1\rangle$	$-i 0\rangle$

The Z gate is a rotation around the Z axis by (Phase gate) which is shown as below:

$$Z = \sigma_z = \begin{pmatrix} 1 & 0 \\ 0 & -1 \end{pmatrix}$$

The following truth table describes the operation rotation around the x axis:

Table 6– Truth table represent z-gate

Input	Output
$ 0\rangle$	$ 0\rangle$
$ 1\rangle$	$- 1\rangle$

The Hadamard (H) gate: The H gate is a frequently used quantum gate that is responsible for putting the qubit's quantum state into a complex linear superposition of its two basis states. This creates the superposition of all qubits used by many quantum algorithms, which is why it is highly popular. The symbol used to represent this gate is H.

$$H = \frac{1}{\sqrt{2}} \begin{pmatrix} 1 & 1 \\ 1 & -1 \end{pmatrix}$$

The truth table shows that the operation results in a rotation of the qubit's state vector by $\pi/2$ (180 degrees) along both the x and z axes. This rotation causes the state vector to be in a complex linear superposition of the $|0\rangle$ and $|1\rangle$ states.

Table 7 – Truth table represent H-gate

Input	Output
$ 0\rangle$	$\frac{ 0\rangle + 1\rangle}{\sqrt{2}}$
$ 1\rangle$	$\frac{ 0\rangle - 1\rangle}{\sqrt{2}}$

There are other gates (S gates, S dagger gate, T gate, T dagger, RF gate) also which are described in Appendix section. There are also universal gates named U1, U2, U3.

Now, we will briefly discuss the multi qubit gate that is called Control-NOT gate that is similar to XOR classical gate. The matrix representation of a CNOT gate is 4×4 matrix due to the tensor product of two qubits:

$$\text{CNOT} = \begin{bmatrix} 1 & 0 & 0 & 0 \\ 0 & 1 & 0 & 0 \\ 0 & 0 & 0 & 1 \\ 0 & 0 & 1 & 0 \end{bmatrix}$$

And the truth table is represented by

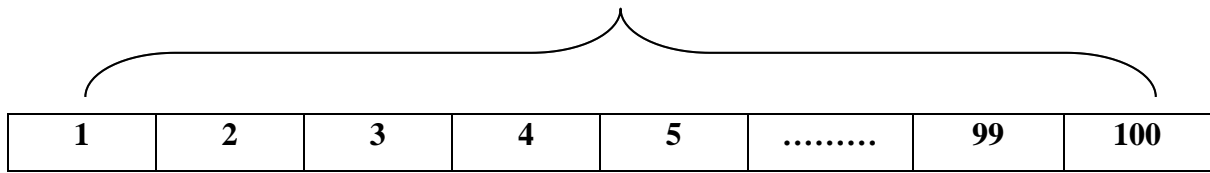
Table 8– Truth table represent CNOT-gate:

Input	Output
$ 00\rangle$	$ 00\rangle$
$ 01\rangle$	$ 01\rangle$
$ 10\rangle$	$ 11\rangle$
$ 11\rangle$	$ 10\rangle$

There are other multi-qubit gates such as Toffoli-multi-qubit (CCX) gate, SWAP gate etc.

3.5.1.1 Description of Quantum Search Algorithm: Grover's search algorithm is known as the quantum search algorithm which solves the problem of unstructured search with high probability. Here we consider below example :

100 Total options
Worst case: requires 99 calls to the classical oracle



In order to find a random value between 1 to 100 attempts 99 times worst classically (N) times. Using Grover's algorithm takes the advantage of qubit in superposition and phase interference to improve unstructured database search from N to \sqrt{N} . From the above example, it takes only $\sqrt{N} = \sqrt{100} = 10$ times. This is quadratic speed up for many classical problems. Grover's search algorithm has two primary components, or possibly three if you include the initialization of all qubits into superposition and measurement at the end. However, these are standard practices in most quantum algorithms, so we will focus on the two main components. The first component is known as Grover's oracle, while the second is called the Grover diffusion operator. We will describe a two-qubit system that placed in superposition by placing a Hadamard gate to each qubit, provides states- 00, 01, 10, 11 as follows :

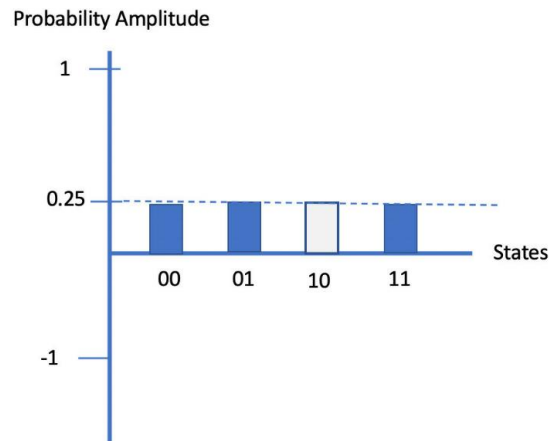


Figure 6: Two qubit in a superposition state

In this state, the average value is equal to the probability amplitude, which is represented by a dotted line at the top of each state and is equal to 0.25 in this particular case. For this example, we want to find the state '10'. The first component is oracle, U_f which simply changes the sign

of the state from positive to negative.

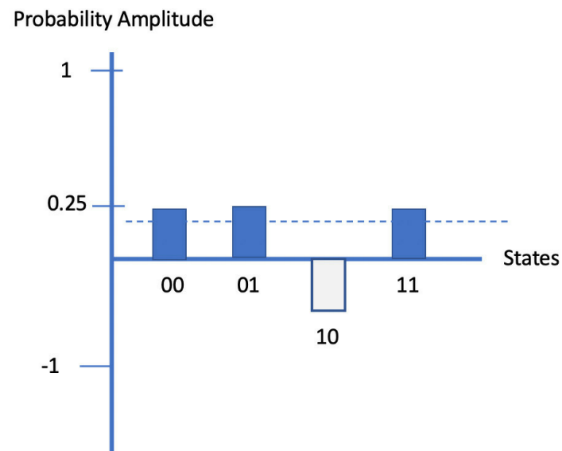


Figure 7 : Changing the sign of the state to negative.

The second component is the Grover diffusion operator which will perform a mathematical step known as inversion about the mean.

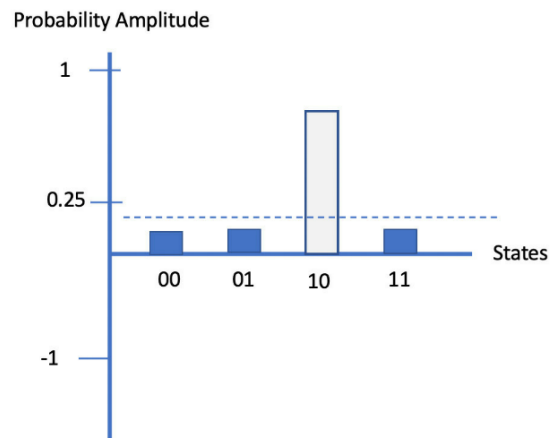


Figure 8 : Inversion about the mean operation

After performing the inversion about the mean, it is apparent that the amplification of the tagged state has increased considerably compared to the other states. If a measurement is taken now, the state with the highest probability is the one that we were searching for.

3.5.2 Quantum Weighted Search Algorithm

3.5.2.1 Basic Complex Function for Hamiltonian Construction

Before conducting CH selection through Quantum Weighted Search Algorithm (QSA), we must discuss the basics of the weighted Grover's search algorithm. Grover's searching algorithm based on weighted targets, each target is endowed with a weight coefficient according to its importance. Applying these different weight coefficients, the targets are represented as quantum superposition states. Using this algorithm, the probability of getting each target can be approximated to the corresponding weight coefficient, which shows the flexibility of this algorithm. We want to search for one specific item in a search space that consists of N elements. For instance, we assume $N = 2^n$, which states that the index of the search items can be kept to n bits. Additionally, the search problem has exactly M solutions within the range of $1 \leq M \leq N$. The algorithm starts with the state: $|0\rangle^{\otimes n}$. This $|0\rangle^{\otimes n}$ state which can be transformed into a superposition state via Walsh–Hadamard transformation [34]:

$$|\phi\rangle = \frac{1}{\sqrt{N}} (|0\rangle + |1\rangle + |q_1\rangle + \dots + |q_M\rangle + \dots + |N-1\rangle) \quad (16)$$

Where $|q_1\rangle, |q_2\rangle \dots |q_M\rangle$ are the marked states, and the set is $Q = \{q_1, q_2, \dots, q_m\}$. If these marked states have weighted coefficients, which are denoted as $w_{q_1}, w_{q_2} \dots w_{q_m}$, they must satisfy $\sum_{i \in Q} w_i = 1$, $w_i > 0$ and the denoted degree of significance of each search items. From [26] it can be written as

$$|q\rangle = \sum_{i=1}^{N-1} c_i |i\rangle = \begin{cases} \sum \sqrt{w_i} |i\rangle \\ 0 |i\rangle \end{cases} \quad (17)$$

Based on equation 17, Oracle operator can be stated as follows,

$$O = I - 2 |q\rangle \langle q| \quad (18)$$

After assigning the weight coefficients in the equation (16) can be represented in to following expression,

$$|\Phi\rangle = x_0 |0\rangle + x_1 |1\rangle + x_{q_1} |q_1\rangle + \dots + x_{q_M} |q_M\rangle + \dots + x_{q_{N-1}} |N-1\rangle = \sum_{i=1}^{N-1} x_i |i\rangle \quad (19)$$

Using the oracle operator O in the equation (19) gives,

$$\begin{aligned}
O &= |\Phi\rangle\langle\Phi| [I - 2|q\rangle\langle q|] \\
&= |\Phi\rangle\langle\Phi| - (2|q\rangle\langle q|)|\Phi\rangle\langle\Phi| \\
&= |\Phi\rangle\langle\Phi| - 2|q\rangle\langle q|\Phi\rangle \\
&= \sum_{i=1}^{N-1} x_i|i\rangle\langle i| - 2 \sum_{i=1}^{N-1} c_i|i\rangle\langle i| \langle q|\Phi\rangle
\end{aligned} \tag{20}$$

[putting the values from equation 17 and 19]

The iterative equation can be constructed from [35] , first sub-step of the superposition becomes

$$|\Phi\rangle^{(t+\frac{1}{2})} = \sum_{i=1}^{N-1} x_i^{(t)}|i\rangle - 2 \sum_{i=1}^{N-1} c_i|i\rangle \langle q|\Phi\rangle^{(t)} \tag{21}$$

And the 2nd sub step of the equation is

$$|\Phi\rangle^{(t+1)} = 2 \sum_{i=1}^{N-1} \langle \Phi^{(t+\frac{1}{2})} | i \rangle |i\rangle - \sum_{i=1}^{N-1} x_i^{(t+\frac{1}{2})} |i\rangle \tag{22}$$

Now, Inserting the value of $|\Phi\rangle^{(t+\frac{1}{2})}$ in equation 22, we can get,

$$|\Phi\rangle^{(t+1)} = 2(\sum_{i=1}^{N-1} \langle x_i^{(t)} - 2\langle q|\Phi\rangle^{(t)} | c_i \rangle) |i\rangle - x_i^{(t)} + 2 \sum_{i=1}^{N-1} c_i|i\rangle \langle q|\Phi\rangle^{(t)} \tag{23}$$

The above term $\langle q|\Phi\rangle^{(t)}$ expression can be written by following assumptions,

$$\langle q|\Phi\rangle^t = V \sin(\omega t + \varphi) \tag{24}$$

The parameters of equation 24 obtained as,

$$V=1 \tag{25}$$

$$\omega = 2 \arcsin(\langle q|\Phi\rangle) \tag{26}$$

$$\varphi = \arcsin(\langle q|\Phi\rangle) \tag{27}$$

If $|\Phi\rangle$ state is equal to the superposition state $|q\rangle$ after some iterations, then the success probability should be equal to 1 that means $(\langle q|\Phi\rangle)^2 = 1$. The success probability can be illustrated after t times of Grover iterations by,

$$t = CI \left(\frac{\pi - \varphi}{\omega} \right) = CI \left(\frac{\arccos \langle q|\Phi\rangle}{2 \arcsin \langle q|\Phi\rangle} \right) \quad (28)$$

Where, CI means integer closest to real number.

In terms of security perspective, the quantum algorithm is more reliable than the classical algorithm is [47,48]. Quantum algorithms are superior to their classical analogues when the input exists in a superposition state. In our case, all of the node information is encrypted in the superposition state which ensures a high degree of security [49].

3.5.2.2 Illustrative example of Quantum Weighted Search Algorithm

In our proposed quantum weighted algorithm, as mentioned before, the limitations on the number of qubits are the main obstacles in quantum computing systems. Therefore, we only used an $n = 4$ qubit system to simulate the performance of our proposed quantum algorithm. Before approaching the quantum part, it is worth mentioning that in some previous research of clustering algorithms, such as EECS, all of the nodes need to send a message to the BS, and the CH needs to send at least three messages, which heavily increases the overhead complexity. Under HEED, a CH probably generates at least N iterations, which is a similar range of time complexity: $O(N)$. Our main approach to implementing a quantum algorithm for CH selection is to reduce the time and overhead complexity. In a quantum computing system, CH selection can be achieved from one to two iterations using Grover's weighted search algorithm, which reduces overhead complexity to $O(\sqrt{N})$.

The above-mentioned nodes, $N = 16 = 2^4$, can be formed into a superposition state with four qubits. Therefore, the initial state can be written from Equation (16):

$$|\Phi\rangle = \frac{1}{\sqrt{16}} (|0000\rangle + |0001\rangle + |0010\rangle \dots \dots \dots + |1111\rangle)$$

where $|0000\rangle, |0001\rangle, |0010\rangle, \dots |1111\rangle$ represent node 1, node 2, node 3, ... node 16, respectively. Our probable CHs are node 10 and node 13 which is the marked state. Grover's

algorithm will search for this marked state within one iteration, which can be proven by the mathematical formulation and IBM's QISKIT quantum simulation.

In the classical CWCA algorithm, the nodes with the lowest weights, node 10 and node 13, will be eligible for CH selection. However, in a quantum algorithm, the highest weighted node will be selected as the CH. Therefore, to select the CH in the quantum approach, all of the nodes' corresponding weights need to be inverted, which is called inversion about the mean. In this process, the nodes' average weights will be calculated, and then, each node's corresponding weight is subtracted from two times the average value. By this process, we obtain new values for the nodes. From Table 9, we can see that the lowest weight nodes become the highest weighted ones. The target that needs to be found must be the node that has the highest weight under Grover's search algorithm. Using the traditional search algorithm, the complexity is linear, but Grover's search algorithm will predict comparatively better complexity. In terms of function, the above expression becomes:

Table 9. Quantum algorithm based on weighted targets parameters and its implementation.

Node ID	Node State	Node weights (W_i)	Inversion about the mean value $W_{inv} = 2*W_i + W_{avg}$
1	0000⟩	1.23	1.27
2	0001⟩	1.20	1.30
3	0010⟩	1.60	0.90
4	0011⟩	2.10	0.40
5	0100⟩	0.85	1.65
6	0101⟩	0.90	1.60
7	0110⟩	1.20	1.30
8	0111⟩	0.90	1.60
9	1000⟩	1.60	0.90
10	1001⟩	0.70	1.80
11	1010⟩	1.90	0.60
12	1011⟩	1.70	0.80
13	1100⟩	0.75	1.75
14	1101⟩	0.78	1.72
15	1110⟩	1.37	1.13
16	1111⟩	Null	Null
Average weights		$W_{avg} = 1.25$	$W_{inv_avg} = 1.25$

$$f(x) = \begin{cases} 1, & \text{if the weight is highest} \\ 0, & \text{if the weight is lowest} \end{cases}$$

Since, Grover's algorithm based on weighted targets requires.

$$\sum_{i=1}^n \omega_i = 1 \quad (30)$$

it means the sum of all of the search target node weights should be one. To obtain the sum value of one, it is necessary to normalize the corresponding weight values. Normalization can be performed via the following formula:

$$\omega_i = \frac{W_{inv}}{\sum_{i=1}^n W_{inv}} \quad (31)$$

where n is the number of candidate nodes. From Table 9, we can see that our candidate nodes are 10 and 13. The sum of their inverted weights is 3.55. As a result, when the normalized weights of node 10 ($w_{10}=0.51$) and node 13 ($w_{13}=0.49$) are added together, they equals one. As mentioned earlier, Equation (16) represents the initial state of the nodes. Our marked state is constructed as follows:

$$|q\rangle = \sqrt{0.51}|1001\rangle + \sqrt{0.49}|1100\rangle \quad (32)$$

Now, the iteration steps can be found with Equation (28) by applying the original Grover's algorithm, which comes from [50]:

$$t = CI \left(\frac{\frac{\pi}{2} - \varphi}{\omega} \right) = CI \left(\frac{\arccos \sqrt{\frac{m}{N}}}{2 \arcsin \sqrt{\frac{m}{N}}} \right) \quad (33)$$

where m = number of candidate nodes/CH nodes, and N = total number of maximum nodes.

Table 10 shows that when comparing both iteration values, Equation (28) depicts a value that is closer to two. Therefore, it can be stated that the targets from Grover's weighted search algorithm are more perfect than the original Grover's search algorithm ones are.

Table 10. Iterations steps for finding the target nodes.

Angular Frequency ω	Phase Angle φ	Iteration Steps by equation (28) t_0	Iteration Steps by equation (33)
0.6908	0.3454	1.77 ~ 2	1.60

CHAPTER 4

Performance Evaluation on classical and Quantum Approach

4.1 Classical Approach

In this section, we discuss the classical clustering performance evaluation in terms of transmission range with fixed node densities and the trade off between the number of cluster and transmission range. We then calculate the energy consumption of intra and inter cluster communication.

4.1.1 Transmission Range for fixed network area with different node densities

First, we discuss the classical clustering performance evaluation. We are interested in optimizing the transmission range, which depends highly on node density. In a WSN, the nodes are stationary after deployment, but it is necessary to deploy sensor nodes wisely because, in our network model, we introduce the network connectivity equation as a function of the transmission range, which is related to node density and the number of sensor nodes in each cluster.

From Table 11, we can see that the relationship between the expected number of clusters and the transmission range is reciprocal. The transmission range r_{tx} needs to be higher if the expected number of clusters decreases. If we can change the network area, for example $A = 100 \text{ m} \times 100 \text{ m}$ in Table 11, and if the number of nodes is 100, the node density will be 0.01 m^{-2} , which is an increase from the previous node density. According to the calculation, the transmission range has decreased from 34 m to 17 m, but the number of clusters remains the same. This illustration, along with data from Table 11, demonstrates how the transmission range will decrease as node density increases.

Table 11. Transmission range for fixed Network area and different node density. (Probability of connectivity considered 0.99)

Network Area (A) m^2	No. of sensor node (N)	Node density (ρ) m^{-2}	Expected number of clusters	Transmission range (r_{tx}) m
200 x 200	500	0.0125	46	16.59
	450	0.01125	42	17.40
	400	0.01	38	18.36
	350	0.00875	33	19.51
	300	0.0075	29	21
	250	0.00625	25	22.70
	200	0.005	20	25
	150	0.00375	16	29
	100	0.0025	11	34
	50	0.0013	6	47

Figure 9 (a) shows the relationship between the total number of sensor nodes and transmission range. When the number of clusters increases, transmission range decreases that is depicted in Figure 9 (b).

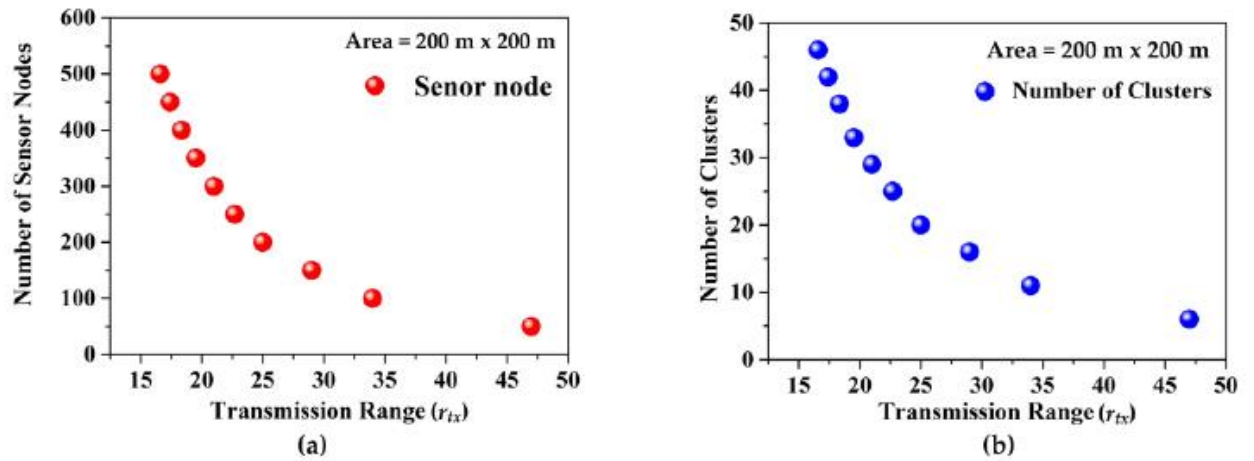


Figure 9. (a) The relationship between the number of sensor nodes and transmission range. And (b) the number of clusters and transmission range.

4.1.2 Energy Calculation for intra and Cluster head to BS communications

In a practical sense, the selection of the optimum number of clusters should be energy efficient and consume low levels of power. In order to select energy-efficient cluster heads, it is essential to calculate the energy consumption between the CH and its member nodes, which is referred to as intra-cluster communications, and between the CH and the BS, which is inter-cluster communications. In the next step, we must characterize intra- and inter-cluster energy consumption, and determine how much energy is saved for different cluster formations through the energy model discussed in Section 3.2. It is worth depicting how, in a cluster, the node consuming the most energy is the CH because it needs to gather information from its member nodes, aggregate their data, and then send them directly to the BS (in our model, we assume that there is single-hop communication with the BS). For this reason, we show the energy dissipation of each member node and the CH separately. In our energy calculation, the power levels of data from the Berkeley CC2420 chip set [51] are used. Before starting the computation, some parameters (showed in Table 6) need to be set ($E_{elec} = 50$ nJ/bit, $e_{fs} = 10$ pJ/bit/m² and $e_{mp} = 0.0013$ pJ/bit/m⁴, $E_{DA} = 5$ pJ/bit per signal) from [35]

Table 12. Computation parameters and values

Parameters	Values
Sensing Region	200 * 200 m ²
N	50
E_{elec}	50 nJ/bit
e_{fs}	10 pJ/bit/m ²
e_{mp}	0.0013 pJ/bit/m ⁴
E_{DA}	5 nJ/bit/signal
Data packet size (l)	1packet = 800 bits

We consider that one cluster has eight member nodes which need to send one packet of data to the corresponding CH. Therefore, each member node's transmission energy per packet can be calculated from Equation (8): 43.2 μ J/packet (distance to the CH, $d_{to\ CH} = 20$ m). In intra-cluster communications, the CH receives a total of eight packets from its member nodes, which consumes 3200 μ J, as calculated from Equation (6). The total energy consumption of intra-

cluster communications is shown in Table 13.

Table 13. Energy calculation of Intra cluster communication

No. of Clusters	No of member node in one cluster	Average distance from member node to CH (Assumption)	Transmission energy [E_{Tx} (μ J)]/packet]from member node	Transmission Energy E_{Tx} (μ J) from one cluster	Receiving Energy E_{Rx} (μ J) of CH from one cluster	Total Energy in cluster (Milli Joule)	Energy Savings (Percentage, %)
1	50	90	104.8	5240	20000	25.24	1%
2	25	85	97.84	2445	10000	12.45	51%
3	16	60	73.8	1181	6400	7.58	70%
4	¹ 12	50	60.6	720	4800	5.52	78%
5	10	30	47.2	472	4000	4.47	82%
6	8	20	43.2	346	3200	3.55	86%

Table 13 clearly shows that as the number of clusters increases, energy consumption decreases, just as energy savings increase in the network. The next step for energy consumption is from the CH to the BS, (inter-cluster energy consumption). From Equation (7), CH energy consumption can be calculated. The total inter-cluster energy consumption is shown in Table 14.

Table 14. Energy calculation of CH to BS communication.

No. of Clusters	No of member node in one cluster	Non-CH node (m-1)	Average distance from CH to BS (meters) [Assumptions]	Transmission energy of CH per cluster (Milli Joule)	Energy Savings (Percentage, %)
1	50	49	20	110.01	1%
2	25	24	25	27.51	75%
3	16	15	30	11.28	89%
4	¹ 12	11	35	6.35	94%
5	10	9	40	4.43	96%
6	8	7	45	2.85	97%

We note that the transmission power level should be at a maximum value for inter-cluster communications. From Table 14, we can see that very low inter-cluster transmission energy is required if the number of clusters increases. Therefore, in both intra- and inter-cluster communications, energy savings is at the highest level when the cluster size increases.

4.1.3 Performance evaluation in terms of optimum number of clusters

Here, we need to consider Berkeley CC2420 chipset again for energy calculations between intra cluster communication (member to CH) and CH to BS station for 15 nodes for exactly to compare the same performance evaluation through quantum algorithm [because for qubit limitation we can only consider highest 16 nodes in quantum search algorithm]. The parameters are considered same without the sensing area that is depicted in Table 15:

Table 15. Computation parameters and values for optimum number of clusters

Parameters	Values
Sensing Region	50 * 50 m ²
N	50
E_{elec}	50 nJ/bit
e_{fs}	10 pJ/bit/m ²
e_{mp}	0.0013 pJ/bit/m ⁴
E_{DA}	5 nJ/bit/signal
Data packet size (l)	1packet = 800 bits

Table 16. Energy calculation of Intra cluster communication in 50 x 50 m² Area

No. of Clusters	No of member node in each cluster	Average distance from member node to CH (Assumption)	Transmission energy [E_{Tx} (μJ)]/packet]from member node	E_{Tx} × number of cluster energy (μJ)	Receiving Energy E_{Rx} (μJ) of CH from one cluster	E_{Rx} × number of cluster energy (μJ)	Total Energy Consumption = $E_{Tx} + E_{Rx}$ (μJ)
1	15	18	638.88	638.88	1693.5	1693.50	2332.38
2	7	15	292.60	585.20	790.3	1580.60	2165.80
3	5	13	206.76	620.28	564.5	1693.50	2313.78
4	3.75	11	153.63	614.52	423.375	1693.50	2308.02
5	3	14	124.70	623.52	338.7	1693.50	2317.02
6	2.5	8	101.28	607.68	282.25	1693.50	2301.18
7	2.2	17	93.09	651.60	248.38	1738.66	2390.26
8	1.8	14	74.82	598.58	203.22	1625.76	2224.34
9	1.6	13	66.16	595.47	180.64	1625.76	2221.23
10	1.5	8	60.77	607.68	169.35	1693.50	2301.18
11	1.36	12	55.97	615.63	153.544	1688.98	2304.62
12	1.25	9	50.81	609.72	141.125	1693.50	2303.22
13	1.15	10	46.92	609.96	129.835	1687.86	2297.82
14	1.07	10	43.66	611.18	120.803	1691.24	2302.43
15	1	12	41.15	617.28	112.9	1693.50	2310.78

In Table 16, there are shown calculations of energy of inter cluster communication for 15 nodes. When the number of clusters is 2, then we have found the lowest energy consumption 2166 μJ . In Table 17, the energy consumption between cluster head (CH) and Base station are also calculated. The total energy consumption found minimum 617 μJ if the cluster number is 2. Therefore, it can be stated that total energy consumption is the lowest when the optimum number of clusters is 2.

Table 17. Energy calculation of Cluster head to Base Station (CH to BS) communication in 50 x 50 m² Area.

No. of Clusters	No of member node in one cluster	Non-CH node (m-1)	Average distance from CH to BS (meters) [Assumptions]	Transmission energy of CH per cluster (μJ)	Total Energy consumption = No. of Cluster \times per cluster energy (μJ)
1	15	14	20	660.17	660.17
2	7	6	22	308.24	616.49
3	5	4	25	220.41	661.22
4	3.75	2.75	25	165.41	661.63
5	3	2	28	132.64	663.20
6	2.5	1.5	26	110.48	662.85
7	2.2	1.2	23	97.09	679.64
8	1.8	0.8	25	79.61	636.85
9	1.6	0.6	28	71.04	639.35
10	1.5	0.5	27	66.55	665.53
11	1.36	0.36	23	60.13	661.44
12	1.25	0.25	29	55.74	668.83
13	1.15	0.15	25	51.01	663.08
14	1.07	0.07	19	47.22	661.02
15	1	0	20	44.17	662.50

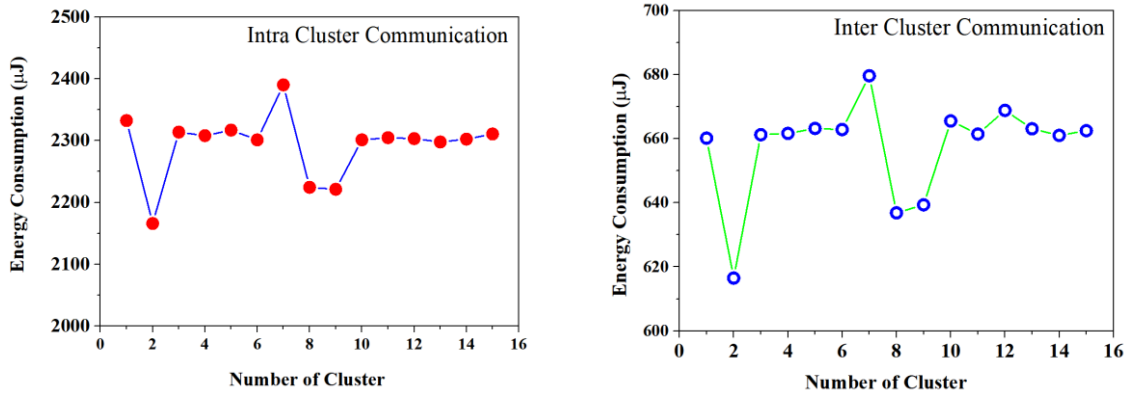


Figure 10: Optimum number of clusters in (a) Intra-Cluster & (b) CH to BS communication.

In Figure 10, (a) and (b) shows the minimum energy consumption in Intra cluster communication and CH to BS communication respectively when the cluster number is 2.

4.2 Quantum Approach

The second phase of the performance evaluation shows the results from the CH selection formulated using Grover's weighted search algorithm in IBM's quantum simulator (QISKIT). In the initialization of this algorithm, the quantum states $|0\rangle^{\otimes n}$ and $|1\rangle$ are set to an equal superposition state, which can be achieved by implementing a Hadamard gate (H) for each qubit.

4.2.1 IBM Quantum Simulator Results and Discussions

For this simulation, the algorithm needs five qubits, where one qubit (q_4) represents an ancilla/auxiliary qubit that is initialized to state $|1\rangle$ by applying a NOT (X) gate, as shown in Figure 11(a). After the implementation of the Hadamard gate (H), the amplitude can be represented by $\frac{1}{\sqrt{N}}$. The next step is to build an Oracle to mark the state. This Oracle can be made by a CZ gate which is a combination of a Hadamard gate and a controlled X (CNOT) gate for a two-qubit system. Our required target states are $|1001\rangle$ and $|1100\rangle$, which represent node 10 and node 13. Therefore, to build an Oracle with four qubits, we need to use a quadruple-controlled (cccc-X) gate that can be constructed using a Multi-Controlled Toffoli (MCT) gate, as shown in Figure 11(b). Then, we build the circuit by creating a superposition

of all of the states, and the final (ancilla) qubit needs to be placed in the $|-\rangle$ state (negative), as required.

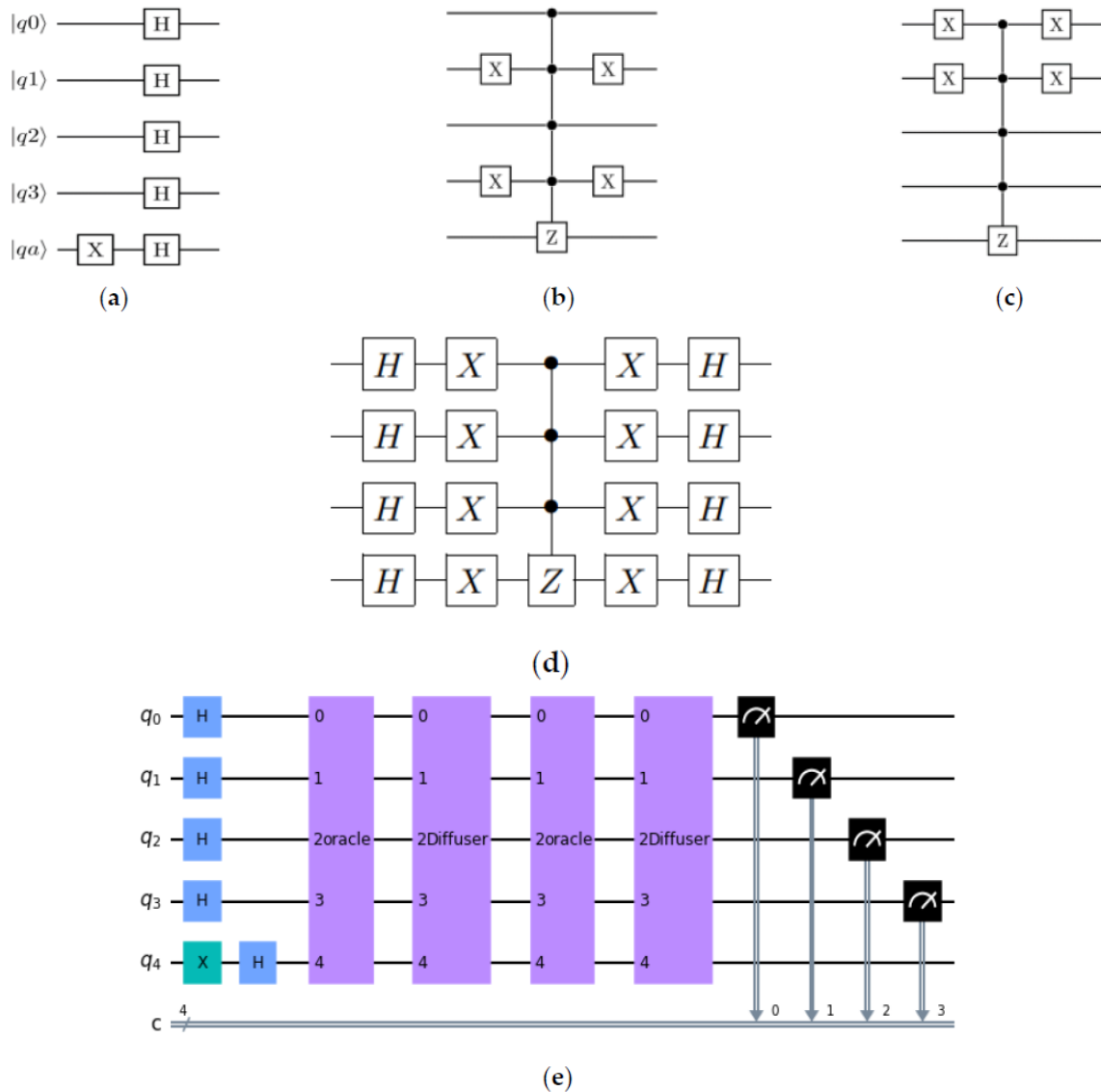


Figure 11. (a) Initialization of the quantum circuit; (b, c) represent Oracle marked states $|1001\rangle$ and $|1100\rangle$ (Note: the #1100 element is marked as (lsb to msb)); (d) the diffusion operator to invert the mean; (e) the complete quantum circuit ready to run on a simulator or quantum system to find the target element with high probability

The next stage in Grover's algorithm is related to implementing a diffuser, which is also called the amplification stage, which inverts the average of the amplitudes. This can be accomplished using the formula HRH , in which H is the Hadamard transform, and R is a phase shift transform

[41]. The amplitudes of the N possible states associated with the newly decreased mean are inverted by a diffuser. The target state's negative phase is reversed by this inversion, which also contributes to differentiating the target from the other states. The last and final step is the measurement of the qubits. After conducting this measurement, the qubits are not in the superposition state, and they collapse to give the outcome of one of the possible states.

The execution of the proposed quantum algorithm is performed on IBM's QasmSimulator, with the results being shown in Figure 12. The marked states are found within $(t_0) = 2$ iterations with 1024 shots, as shown in Figure 12a. If we increase the number of shots to 8192, then the probability of finding the states remains the same at the highest values of the two states.

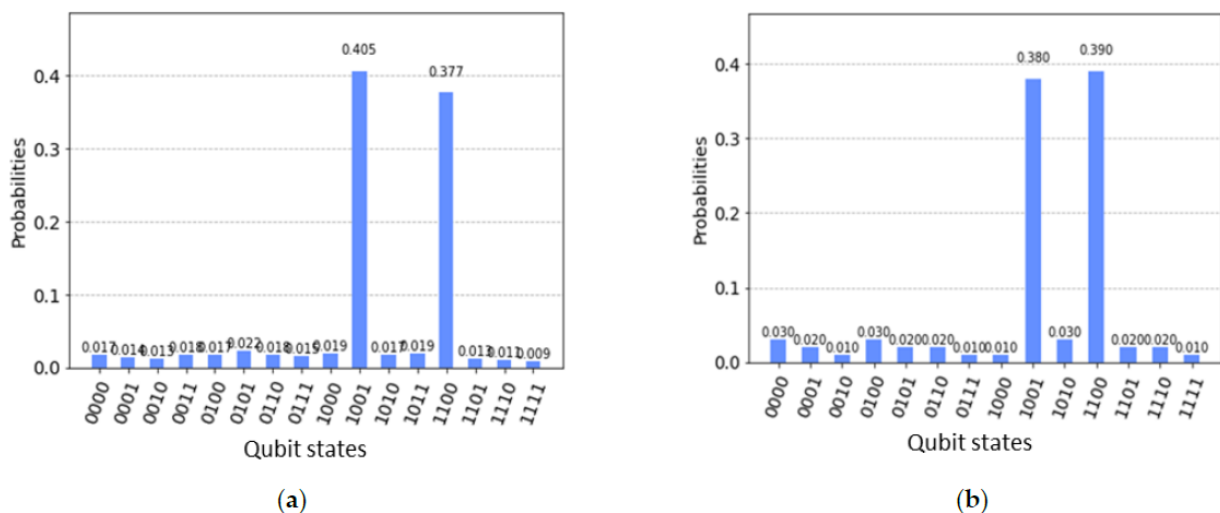


Figure 12. (a) QasmSimulator results when the number of shots = 1024, and (b) when the number of shots = 8192.

The above results indicate that for the two states, $|1001\rangle$ and $|1100\rangle$, the probabilities are 40% and 37%, respectively, which means if we run the algorithm every time, the two states will have the highest probability. Within two iterations, we will reach our probable destination. There are negligible discrepancies between the theoretical values of the iterations and the simulation results because if we increase the iteration values in the simulator, then the probability of success will increase by around 10%, but we can still obtain the same state with the same results. Therefore, we can state that with the two single Grover's operator, the desired

results can be found. The maximum number of iterations for this experiment is $O(\frac{\pi}{4}\sqrt{N})$, where $N = 16$ nodes. However, here, we can see that within two iterations, we can find our target state. If we increase the number of iterations (t_0) of Grover's operator, the algorithmic success probability (ASP) will be high. In the classical algorithm, in order to find the search state, we need to check each value (in the worst case) for the required time complexity $O(N)$. For time complexity, the quantum algorithm surpasses the classical algorithm in terms of the CH selection procedure. In sum, this reduction in time will improve the overall performance of the network by decreasing the end-to-end delay and power consumption.

CHAPTER 5

Conclusions

This paper introduced an optimization approach for a WSN-based hierarchical network with the focus on topology control as a function of the transmission range and power. A novel approach to cluster head selection (in both classical and quantum computing) attributed to transmission power will help to establish an energy-efficient network. The factors (the node degree, average distance between nodes, and energy consumption) which are essential for CH selection and proposed for the CWCA algorithm are scalable in terms of weight. MATLAB simulations of the classical algorithm show that around 86% and 97% of the energy efficiency is achievable in the whole network for intra- and inter-cluster communications, respectively. On the other hand, by reducing the time complexity and with a faster search for CH selection, an improved weighted target-based quantum search algorithm was proposed. By implementing the QWSA algorithm, the cluster head can be selected within two iteration steps, which is a favourable agreement between the mathematic approach and the QISKIT simulation result.

A probable limitation of the CWCA technique is that it requires a computationally expensive system when considering a large number of cluster heads. It will also be necessary to evaluate the end-to-end reliability and the delay in the sensor data. In addition, it is essential to ensure security in the cluster head selection process such as identify selfish and duplicate nodes. Future research directions will focus on implementing the proposed QWSA algorithm in significant networking systems. Now, the performance is bounded because of the limited number of qubits. For instances, if we increase the number of qubits by two times, we can easily implement this algorithm for about 256 (2^8) nodes and increasing it by three times the number of qubits in the simulation can cover up to 4096 (2^{12}) nodes in the whole network.

We also demonstrated that qubit selection can have a significant impact on how the quantum algorithms are implemented, and researchers will need to pay attention to this when they are trying to accurately implement algorithms in the future. IBM and other experts in quantum

computing are continuously enhancing and introducing new quantum devices. In the future, it will be essential to follow the development of these new and advanced devices to gain a sense of how rapidly quantum computing technology is progressing.

REFERENCES

1. Maraiya, K.; Kant, K.; Gupta, N. Application Based Study on Wireless Sensor Network. *Int. J. Comput. Appl.* **2011**, *21*, 9–15. <https://doi.org/10.5120/2534-3459>.
2. Majid, M.; Habib, S.; Javed, A.R.; Rizwan, M.; Srivastava, G.; Gadekallu, T.R.; Lin, J.C.W. Applications of Wireless Sensor Networks and Internet of Things Frameworks in the Industry Revolution 4.0: A Systematic Literature Review. *Sensors* **2022**, *22*, 2087. <https://doi.org/10.3390/s22062087>.
3. Yi, F.; Zhang, L.; Xu, L.; Yang, S.; Lu, Y.; Zhao, D. WSNEAP: An Efficient Authentication Protocol For IIoT-Oriented Wireless Sensor Networks. *Sensors* **2022**, *22*, 7413.
4. Deverajan, G.; Ramakrishnan, S. Selfish Node Detection Based on Evidence by Trust Authority and Selfish Replica Allocation in DANET. *Int. J. Inf. Commun. Technol.* **2016**, *9*, 473. <https://doi.org/10.1504/IJICT.2016.079961>.
5. Raghunathan, V.; Schurgers, C.; Park, S.; Srivastava, M.B. Energy-Aware Wireless Microsensor Networks. *IEEE Signal Process. Mag.* **2002**, *19*, 40–50. <https://doi.org/10.1109/79.985679>.
6. Behera, T.M.; Samal, U.C.; Mohapatra, S.K.; Khan, M.S.; Appasani, B.; Bizon, N.; Thounthong, P. Energy-Efficient Routing Protocols for Wireless Sensor Networks: Architectures, Strategies, and Performance. *Electronics* **2022**, *11*, 2282. <https://doi.org/10.3390/electronics11152282>.
7. Palanisamy, S.; Sennan, S.; Ramasubbareddy, S.; Deverajan, G. Communication Trust and Energy-Aware Routing Protocol for WSN Using D-S Theory. *Int. J. Grid High Perform. Comput.* **2021**, *13*, 24–36. <https://doi.org/10.4018/IJGHPC.2021100102>.
8. Jibreel, F.; Tuyishimire, E.; Daabo, M.I. An Enhanced Heterogeneous Gateway-Based Energy-Aware Multi-Hop Routing Protocol for Wireless Sensor Networks. *Information* **2022**, *13*, 166. <https://doi.org/10.3390/info13040166>.
9. Schwieger, K.; Fettweis, G. Multi-Hop Transmission: Benefits and Deficits. In *2. Fachgesprach der GI/ITG Fachgruppe KuVS" Drahtlose Sensornetze" 26./27. Februar*

- 2004 *Universität Karlsruhe (TH)*; Institute of Telematics, University of Karlsruhe, Zirkel 2, D-76128 Karlsruhe, Germany. 2004.
10. Wu, M. An Efficient Hole Recovery Method in Wireless Sensor Networks. In Proceedings of the 2022 24th International Conference on Advanced Communication Technology (ICACT), PyeongChang Kwangwoon_Do, Republic of Korea, 13–16 February 2022; pp. 1399–1404. <https://doi.org/10.23919/ICACT53585.2022.9728957>.
 11. Fedor, S.; Collier, M. On the Problem of Energy Efficiency of Multi-Hop vs One-Hop Routing in Wireless Sensor Networks. In Proceedings of the 21st International Conference on Advanced Information Networking and Applications Workshops (AINAW'07), Niagara Falls, ON, Canada, 21–23 May 2007; Volume 1, pp. 380–385. <https://doi.org/10.1109/AINAW.2007.272>.
 12. Sabet, M.; Naji, H.R. A Decentralized Energy Efficient Hierarchical Cluster-Based Routing Algorithm for Wireless Sensor Networks. *AEU—Int. J. Electron. Commun.* **2015**, *69*, 790–799. <https://doi.org/10.1016/j.aeue.2015.01.002>.
 13. Shagari, N.M.; Bin Salleh, R.; Ahmedy, I.; Idris, M.Y.I.; Murtaza, G.; Ali, U.; Modi, S. A Two-Step Clustering to Minimize Redundant Transmission in Wireless Sensor Network Using Sleep-Awake Mechanism. *Wirel. Networks* **2022**, *28*, 2077–2104. <https://doi.org/10.1007/s11276-021-02885-8>.
 14. Shakhov, V.; Koo, I. An Efficient Clustering Protocol for Cognitive Radio Sensor Networks. *Electronics* **2021**, *10*, 84. <https://doi.org/10.3390/electronics10010084>.
 15. Rawat, P.; Chauhan, S. Clustering Protocols in Wireless Sensor Network: A Survey, Classification, Issues, and Future Directions. *Comput. Sci. Rev.* **2021**, *40*, 100396. <https://doi.org/10.1016/j.cosrev.2021.100396>.
 16. Mohan, P.; Subramani, N.; Alotaibi, Y.; Alghamdi, S.; Khalaf, O.I.; Ulaganathan, S. Improved Metaheuristics-Based Clustering with Multihop Routing Protocol for Underwater Wireless Sensor Networks. *Sensors* **2022**, *22*, 1618. <https://doi.org/10.3390/s22041618>.

17. Han, B.; Ran, F.; Li, J.; Yan, L.; Shen, H.; Li, A. A Novel Adaptive Cluster Based Routing Protocol for Energy-Harvesting Wireless Sensor Networks. *Sensors* **2022**, *22*, 1564. <https://doi.org/10.3390/s22041564>.
18. Krishnasamy, L.; Dhanaraj, R.K.; Ganesh Gopal, D.; Reddy Gadekallu, T.; Aboudaif, M.K.; Abouel Nasr, E. A Heuristic Angular Clustering Framework for Secured Statistical Data Aggregation in Sensor Networks. *Sensors* **2020**, *20*, 4937. <https://doi.org/10.3390/s20174937>.
19. Gong, Y.; Lai, G. Low-Energy Clustering Protocol for Query-Based Wireless Sensor Networks. *IEEE Sens. J.* **2022**, *22*, 9135–9145. <https://doi.org/10.1109/JSEN.2022.3159546>.
20. Ye, M.; Li, C.; Chen, G.; Wu, J. An Energy Efficient Clustering Scheme in Wireless Sensor Networks. *Ad-Hoc Sens. Wirel. Networks* **2007**, *3*, 99–119.
21. Lin, C.H.; Tsai, M.J. A Comment on “HEED: A Hybrid, Energy-Efficient, Distributed Clustering Approach for Ad Hoc Sensor Networks”. *IEEE Trans. Mob. Comput.* **2006**, *5*, 1471–1472. <https://doi.org/10.1109/TMC.2006.141>.
22. Bettstetter, C. On the Minimum Node Degree and Connectivity of a Wireless Multihop Network. In Proceedings of the 3rd ACM International Symposium on Mobile ad Hoc Networking & Computing, Lausanne, Switzerland, 9–11 June 2002; p. 80. <https://doi.org/10.1145/513810.513811>.
23. Li, X.-Y.; Wang, Y.; Wang, Y. Complexity of Data Collection, Aggregation, and Selection for Wireless Sensor Networks. *IEEE Trans. Comput.* **2011**, *60*, 386–399. <https://doi.org/10.1109/TC.2010.50>.
24. Roy, S.G.; Chakrabarti, A. Chapter 11—A Novel Graph Clustering Algorithm Based on Discrete-Time Quantum Random Walk. In *Quantum Inspired Computational Intelligence*; Bhattacharyya, S., Maulik, U., Dutta, P., Eds.; Morgan Kaufmann: Boston, MA, USA, 2017; pp. 361–389, ISBN 978-0-12-804409-4.

25. Manuel, A.J.; Deverajan, G.G.; Patan, R.; Gandomi, A.H. Optimization of Routing-Based Clustering Approaches in Wireless Sensor Network: Review and Open Research Issues. *Electronics* **2020**, *9*, 1630. <https://doi.org/10.3390/electronics9101630>.
26. Kleinberg, Jon and Tardos, Eva. Algorithmic Design. *kleinberg2006algorithm*, Pearson Education India, 2006.
27. Ushakov, A.V.; Vasilyev, I. A Parallel Heuristic for a K-Medoids Clustering Problem with Unfixed Number of Clusters. In Proceedings of the 2019 42nd International Convention on Information and Communication Technology, Electronics and Microelectronics (MIPRO), Opatija, Croatia, 20–24 May 2019; pp. 1116–1120. <https://doi.org/10.23919/MIPRO.2019.8756919>.
28. Sahoo, B.M.; Amgoth, T.; Pandey, H.M. Particle Swarm Optimization Based Energy Efficient Clustering and Sink Mobility in Heterogeneous Wireless Sensor Network. *Ad Hoc Networks* **2020**, *106*, 102237. <https://doi.org/10.1016/j.adhoc.2020.102237>.
29. Choi, J.; Oh, S.; Kim, J. Energy-Efficient Cluster Head Selection via Quantum Approximate Optimization. *Electronics* **2020**, *9*, 1669. <https://doi.org/10.3390/electronics9101669>.
30. Lee, E. Optimizing Quantum Circuit Parameters via SDP 2022. <https://doi.org/10.48550/arxiv.2209.00789>.
31. Villalba-Diez, J.; González-Marcos, A.; Ordieres-Meré, J.B. Improvement of Quantum Approximate Optimization Algorithm for Max–Cut Problems. *Sensors* **2022**, *22*, 244. <https://doi.org/10.3390/s22010244>.
32. Giri, P.R.; Korepin, V.E. *A Review on Quantum Search Algorithms*; Springer: USA, 2017; Volume 16, ISBN 1112801717687. <https://doi.org/10.1007%2Fs11128-017-1768-7>.
33. Wright, J.; Tseng, T. Lecture 04: Grover's Algorithm. Carnegie Mellon University, Quantum Computation and Information:(15-859BB), **2015**, 1–12.
34. Panchi, L.; Shiyong, L. Grover Quantum Searching Algorithm Based on Weighted Targets. *J. Syst. Eng. Electron.* **2008**, *19*, 363–369. [https://doi.org/10.1016/S1004-4132\(08\)60093-6](https://doi.org/10.1016/S1004-4132(08)60093-6).

35. Heinzelman, W.B.; Chandrakasan, A.P.; Balakrishnan, H. An Application-Specific Protocol Architecture for Wireless Microsensor Networks. *IEEE Trans. Wirel. Commun.* **2002**, *1*, 660–670. <https://doi.org/10.1109/TWC.2002.804190>.
36. Lindsey, S.; Raghavendra, C.S. PEGASIS: Power-Efficient Gathering in Sensor Information Systems. *IEEE Aerosp. Conf. Proc.* **2002**, *3*, 1125–1130. <https://doi.org/10.1109/AERO.2002.1035242>.
37. Li, C.; Ye, M.; Chen, G.; Wu, J. An Energy-Efficient Unequal Clustering Mechanism for Wireless Sensor Networks. In Proceedings of the International Conference on Mobile Adhoc and Sensor Systems Conference, Washington, DC, USA, 7 November 2005; Volume 2005, pp. 597–604. <https://doi.org/10.1109/MAHSS.2005.1542849>.
38. Priyadarshi, R.; Soni, S.K.; Nath, V. Energy Efficient Cluster Head Formation in Wireless Sensor Network. *Microsyst. Technol.* **2018**, *24*, 4775–4784. <https://doi.org/10.1007/s00542-018-3873-7>.
39. Zhu, J.; Wu, C.; Cui, Y.; Li, D.; Zhang, Y.; Xu, J.; Li, C.; Iqbal, S.; Cao, M. Blue-Emitting Carbon Quantum Dots: Ultrafast Microwave Synthesis, Purification and Strong Fluorescence in Organic Solvents. *Colloids Surfaces A Physicochem. Eng. Asp.* **2021**, *623*, 126673. <https://doi.org/10.1016/j.colsurfa.2021.126673>.
40. Iqbal, S.; Amjad, A.; Javed, M.; Alfakeer, M.; Mushtaq, M.; Rabea, S.; Elkaeed, E.B.; Pashameah, R.A.; Alzahrani, E.; Farouk, A.-E. Boosted Spatial Charge Carrier Separation of Binary ZnFe₂O₄/S-g-C₃N₄ Heterojunction for Visible-Light-Driven Photocatalytic Activity and Antimicrobial Performance. *Front. Chem.* **2022**, *10*, 894. <https://doi.org/10.3389/fchem.2022.975355>.
41. Grover, L.K. A Fast Quantum Mechanical Algorithm for Database Search. In Proceedings of the Twenty-Eighth Annual ACM Symposium on Theory of Computing, STOC '96, Philadelphia, PA, USA, 22–24 May 1996.
42. Kim, H.S.; Andersen, M.P.; Chen, K.; Kumar, S.; Zhao, W.J.; Ma, K.; Culler, D.E. System Architecture Directions for Post-SoC/32-Bit Networked Sensors. In Proceedings of the

- 16th ACM Conference on Embedded Networked Sensor Systems, Shenzhen, China, 4–7 November 2018; pp. 264–277. <https://doi.org/10.1145/3274783.3274839>.
43. Bettstetter, C. On the Connectivity of Wireless Multihop Networks with Homogeneous and Inhomogeneous Range Assignment. *IEEE Veh. Technol. Conf.* **2002**, *56*, 1706–1710. <https://doi.org/10.1109/vetecf.2002.1040507>.
 44. Prasai, K.; Ghimire, S. Selection of Weighting Factors in Weighted Clustering Algorithm in MANET. *Lect. Notes Eng. Comput. Sci.* **2016**, *2225*, 101–107.
 45. Ezhov, A.A.; Nifanova, A.V.; Ventura, D. Quantum Associative Memory with Distributed Queries. *Inf. Sci.* **2000**, *128*, 271–293. [https://doi.org/10.1016/S0020-0255\(00\)00057-8](https://doi.org/10.1016/S0020-0255(00)00057-8).
 46. Bushnag, A.; Alessa, A.; Li, M.; Elleithy, K. Directed Diffusion Based on Weighted Grover’s Quantum Algorithm (DWGQ). In Proceedings of the 2015 Long Island Systems, Applications and Technology, Farmingdale, NY, USA, 1 May 2015; pp. 1–5. <https://doi.org/10.1109/LISAT.2015.7160216>.
 47. Biasse, J.-F.; Bonnetain, X.; Kirshanova, E.; Schrottenloher, A.; Song, F. Quantum Algorithms for Attacking Hardness Assumptions in Classical and Post-Quantum Cryptography. *IET Inf. Secur.* **2022**. <https://doi.org/10.1049/ise2.12081>.
 48. Peelam, M.S.; Johari, R. Enhancing Security Using Quantum Computing (ESUQC). In *Proceedings of the Machine Learning, Advances in Computing, Renewable Energy and Communication*; Tomar, A., Malik, H., Kumar, P., Iqbal, A., Eds.; Springer: Singapore, 2022; pp. 227–235.
 49. Chamoli, A.; Bhandari, C.M. Grover’s Algorithm Based Multi-Qubit Secret Sharing Scheme. *arXiv preprint* **2007**, arXiv:0707.1042.
 50. Seo, Y.; Kang, Y.; Heo, J. Quantum Search Algorithm for Weighted Solutions. *IEEE Access* **2022**, *10*, 16209–16224. <https://doi.org/10.1109/ACCESS.2022.3149351>.
 51. Ieee, G.; Transceiver, Z.R.F. Cc2420 Cc2420.
 52. Robert Loredó, “Learn Quantum Computing with Python and IBM Quantum: Write your own practical quantum programs with Python, 2nd Edition”